

1 Simulating Bark Beetle Outbreak Dynamics and their Influence on 2 Carbon Balance Estimates with ORCHIDEE r7791

3
4 Guillaume Marie^{1*}, Jina Jeong^{2*}, Hervé Jactel³, Gunnar Petter⁴, Maxime Cailleret⁵, Matthew J.
5 McGrath¹, Vladislav Bastrikov⁶, Josefine Ghattas⁷, Bertrand Guenet⁸, Anne Sofie Lansø⁹, Kim
6 Naudts¹¹, Aude Valade¹⁰, Chao Yue¹², Sebastiaan Luyssaert²

7
8 ¹ Laboratoire des Sciences du Climat et de l'Environnement, CEA CNRS UVSQ UP Saclay, 91191 Orme des
9 Merisiers, Gif-sur-Yvette, France

10 ² Faculty of Science, A-LIFE, Vrije Universiteit Amsterdam, 1081 BT Amsterdam, the Netherlands

11 ³ INRAE, University of Bordeaux, umr Biogeco, 33612 Cestas, France

12 ⁴ ETH Zürich, Department of Environmental Systems Science, Forest Ecology, 8092 Zürich, Switzerland

13 ⁵ INRAE, Aix-Marseille Univ, UMR RECOVER, 13182 Aix-en-Provence, France

14 ⁶ Science Partner, France

15 ⁷ Institut Pierre-Simon Laplace – Sciences du climat (IPSL), 75105 Jussieu, France

16 ⁸ Laboratoire de Géologie, Ecole Normale Supérieure, CNRS, PSL Research University, IPSL, 75005 Paris, France

17 ⁹ Department of Environmental Science, Aarhus Universitet, Frederiksborgvej 399, 4000 Roskilde, Denmark

18 ¹⁰ Eco & Sols, Univ Montpellier, CIRAD, INRAE, 34060 Institut Agro, IRD, Montpellier, France

19 ¹¹ Department of Earth Sciences, Vrije Universiteit Amsterdam, 1081 HV Amsterdam, the Netherlands

20 ¹² State Key Laboratory of Soil Erosion and Dryland Farming on the Loess Plateau, Northwest A & F University,
21 Yangling, Shaanxi, China

22

23 * These authors contributed equally to this study

24

25 **Corresponding author:** Guillaume Marie, guillaume.marie@lsce.ipsl.fr, Jina Jeong, j.jeong@vu.nl, Sebastiaan
26 Luyssaert, s.luyssaert@vu.nl

27

28 **Abstract** : New (a)biotic conditions, resulting from climate change, are expected to change disturbance dynamics,
29 e.g., wind throw, forest fires, droughts, and insect outbreaks, and their interactions. Unprecedented natural
30 disturbance dynamics might alter the capability of forest ecosystems to buffer atmospheric CO₂ increases in the
31 atmosphere, even leading to the risk that forests transform from sinks into sources of CO₂. This study aims to
32 enhance the capability of the ORCHIDEE land surface model to study the impacts of climate change on bark beetle
33 dynamics and subsequent effects on forest functioning. The bark beetle outbreak model is inspired by previous work
34 from Temperli et al. 2013 for the LandClim landscape model. The new implementation of this model in ORCHIDEE
35 r7791 accounts for the following differences between ORCHIDEE and LandClim: (1) the coarser spatial resolution

36 of ORCHIDEE, (2) the higher temporal resolution of ORCHIDEE, and (3) the pre-existing process representation of
37 windthrow, drought, and forest structure in ORCHIDEE. Simulation experiments demonstrated the model's ability to
38 simulate a wide range of observed post-disturbance forest dynamics. Through an array of simulation experiments
39 across various climatic conditions and disturbance intensities, the enhanced model was rigorously tested for
40 sensitivity. The model accurately mirrored a wide array of observed post-disturbance forest dynamics, including the
41 capacity of forests to resist infestations and variable recovery periods ranging from 7 to 14 years. Notably, the study
42 revealed that incorporating abrupt mortality events into the model, as opposed to a continuous mortality framework,
43 offers profound insights into the short-term carbon sequestration potential of forests under disturbance regimes. This
44 model enhancement underscores the critical need to include disturbance dynamics in land surface models to refine
45 predictions of forest carbon dynamics in a changing climate.

46

47

48

49 **1. Introduction**

50 Future climate will likely bring new abiotic constraints through the co-occurrence of multiple connected hazards,
51 e.g., “hotter droughts”, which are droughts combined with heat waves (Allen et al., 2015; Zscheischler et al., 2018),
52 but also new biotic conditions from interacting natural and anthropogenic disturbances, e.g., insect outbreaks
53 following windthrow or forest fires (Seidl et al., 2017). Unprecedented natural disturbance dynamics might alter
54 biogeochemical cycles specifically the capability of forest ecosystems to buffer the CO₂ increase in the atmosphere
55 (Hicke et al., 2012; Seidl et al., 2014) and the risk that forests are transformed from sinks into sources of CO₂ (Kurz
56 et al., 2008a). The magnitude of such alteration, however, remains uncertain principally due to the lack of impact
57 studies that include disturbance regime shifts at global scale (Seidl et al., 2011).

58

59 Land surface models are used to study the relationships between climate change and the biogeochemical cycles of
60 carbon, water, and nitrogen (Cox et al., 2000; Ciais et al., 2005; Friedlingstein et al., 2006; Zaehle and Dalmonech,
61 2011; Luysaert et al., 2018). Many of these models use background mortality to obtain an equilibrium in their
62 biomass pools. This classic approach towards forest dynamics, which assumes steady-state conditions over long
63 periods of time, may not be suitable for assessing the impacts of disturbances on shorter time scales under a fast
64 changing climate. This could be considered a shortcoming in the land surface models because disturbances can have
65 significant impacts on ecosystem services, such as water regulation, carbon sequestration, and biodiversity (Quillet
66 et al., 2010). Mechanistic approaches that account for a variety of mortality causes, such as age, size, competition,
67 climate, and disturbances, are now being considered and tested to simulate forest dynamics more accurately
68 (Migliavacca et al., 2021). For example, the land surface model ORCHIDEE accounts for mortality from
69 interspecific competition for light in addition to background mortality (Naudts et al., 2015). Implementing a more
70 mechanistic view on mortality is thought to be essential for improving our understanding of the impacts of climate
71 change on forest dynamics and the provision of ecosystem services.

72

73 Land surface models also face the challenge of better describing mortality particularly when it comes to ecosystem
74 responses to “cascading disturbances”, where legacy effects from one disturbance affect the next (Zscheischler et al.,
75 2018; Buma, 2015). Biotic disturbances, such as bark beetle outbreaks, strongly depend on previous disturbances as
76 their infestation capabilities are higher when tree vitality is low, for example following drought or storm events
77 (Seidl et al., 2018). This illustrates how interactions between biotic and abiotic disturbances can have substantial
78 effects on ecosystem dynamics and must be accounted for in land surface models to improve our understanding of
79 the impacts of climate change on forest dynamics (Temperli et al., 2013; Seidl et al., 2011). While progress has been
80 made towards including abrupt mortality from individual disturbance types such as wildfire (Yue et al., 2014;
81 Lasslop et al., 2014; Migliavacca et al., 2013), windthrow (Chen et al., 2018) and drought (Yao et al., 2022), the
82 interaction of biotic and abiotic disturbances remains both a knowledge and modeling gap (Kautz et al., 2018).

83

84 Bark beetle infestations are increasingly recognized as disturbance events of regional to global importance (Kurz et
85 al., 2008b; Bentz et al., 2010; Seidl et al., 2018). Notably, a bark beetle outbreak ravaged over 90% of Engelmann
86 spruce trees across approximately 325,000 hectares in the Canadian and American Rocky Mountains between 2005
87 and 2017 (Andrus et al., 2020). In Europe, the spruce bark beetle, *Ips typographus*, has been involved in up to 8% of
88 total tree mortality due to natural disturbances from 1850 to 2000 (Hlásny et al., 2021a). A recent increase in beetle
89 activity, particularly following mild winters (Kurz et al., 2008b; Andrus et al., 2020), windthrow (Mezei et al.,
90 2017), and droughts (Nardi et al., 2023) have been well-documented (Hlásny et al., 2021a; Pasztor et al., 2014),
91 underscoring the need to integrate bark beetle dynamics into land surface modeling.

92

93 Past studies used a variety of approaches to model the impacts of bark beetles on forests. While some model treated
94 bark beetle outbreaks as background mortality (Naudts et al., 2016; Luysaert et al., 2018), others dynamically
95 modeled these outbreaks within ecosystems (Temperli et al., 2013; Seidl and Rammer, 2016; Jönsson et al., 2012).
96 Studies with prescribed beetle outbreaks tend to focus on the direct effects of the outbreak on forest conditions and
97 carbon fluxes, but are likely to overlook more complex feedback processes, such as interactions with other
98 disturbances and longer-term impacts. Conversely, dynamic modeling of beetle outbreaks, provides a more
99 comprehensive view by incorporating the lifecycle of bark beetles, tree defense mechanisms, and ensuing alterations
100 in forest composition and functionality.

101

102 Simulation experiments for *Ips typographus* outbreaks using the LPJ-GUESS vegetation model highlighted regional
103 variations in outbreak frequencies, pinpointing climate change as a key exacerbating factor (Jönsson et al., 2012).
104 Simulation experiments with the iLand landscape model suggested that almost 65% of the bark beetle outbreaks are
105 aggravated by other environmental drivers (Seidl and Rammer, 2016). A 4°C temperature increase could result in a
106 265% increase in disturbed areas and a 1800% growth in average patch size (Seidl and Rammer 2016). Disturbance
107 interactions were ten times more sensitive to temperature changes, boosting the disturbance regime's climate
108 sensitivity. The results of these studies justify the inclusion of interacting disturbances in land surface models, such
109 as ORCHIDEE, which are used in future climate predictions and impact studies (Boucher et al., 2020).

110

111 The objectives of this study are: (1) to develop and implement a spatially implicit bark beetle (*Ips Typographus*)
112 outbreak model in the land surface model ORCHIDEE inspired by the work from Temperli et al. (2013), and (2) use
113 simulation experiments to characterize the behavior of this newly added model functionality.

114

115 2. Model description

116 2.1. The land surface model ORCHIDEE

117 ORCHIDEE is the land surface model of the IPSL (Institut Pierre Simon Laplace) Earth system model (Krinner et
118 al., 2005; Boucher et al., 2020). ORCHIDEE can, however, also be run off-line as a stand-alone land surface model
119 forced by temperature, humidity, pressure, precipitation, and wind conditions. Unlike the coupled setup, which needs
120 to run on the global scale, the stand-alone configuration can cover any area ranging from a single grid point to the
121 global domain.

122

123 ORCHIDEE does not enforce any particular spatial resolution. The spatial resolution is an implicit user setting that
124 is determined by the resolution of the climate forcing (or the resolution of the atmospheric model in a coupled
125 configuration). ORCHIDEE can run on any temporal resolution. This apparent flexibility is somewhat restricted as
126 processes are formalized at given time steps: half-hourly (e.g., photosynthesis and energy budget), daily (i.e., net
127 primary production), and annual (i.e. vegetation demographic processes). With the current model architecture
128 meaningful simulations should have a temporal resolution of one minute to one hour for the calculation of energy
129 balance, water balance, and photosynthesis.

130

131 ORCHIDEE utilizes meta-classes to describe different types of vegetation. The model includes 13 meta-classes by
132 default, including one class for bare soil, eight classes for various combinations of leaf-type and climate zones of
133 forests, two classes for grasslands, and two classes for croplands. Each meta-class can be further subdivided into an
134 unlimited number of plant functional types (PFTs). The current default setting of ORCHIDEE distinguishes 15 PFTs
135 where the C3 grasslands have now a separate PFT in the boreal, temperate and tropical zone.

136

137 At the beginning of a simulation, each forest PFT in ORCHIDEE contains a monospecific forest stand that is
138 defined by a user-defined but fixed number of diameter classes (three by default). Throughout the simulation, the
139 boundaries of the diameter classes are adjusted to accommodate changes in the stand structure, while the number of
140 classes remains constant. Flexible class boundaries provide a computationally efficient approach to simulate
141 different forest structures. For instance, an even-aged forest is simulated by using a small diameter range between
142 the smallest and largest trees, resulting in all trees belonging to the same stratum. Conversely, an uneven-aged forest
143 is simulated by applying a wide range between diameter classes, such that different classes represent different strata.

144

145 The model uses allometric relationships to link tree height and crown diameter to stem diameter. Individual tree
146 canopies are not explicitly represented, instead a canopy structure model based on simple geometric forms (Haverd

147 et al. 2012) has been included in ORCHIDEE (Naudts et al., 2015). Diameter classes represent trees with different
148 mean diameter and height, which informs the user about the social position of trees within the canopy. Intra-stand
149 competition is based on the basal area of individual trees, which accounts for the fact that trees with a higher basal
150 area occupy dominant positions in the canopy and are therefore more likely to intercept light and thus contribute
151 more to stand-level photosynthesis and biomass growth compared to suppressed trees (Deleuze et al., 2004). If
152 recruitment occurs, diameter classes evolve into cohorts. However, in the absence of recruitment, all diameter
153 classes contain trees of the same age.

154

155 Individual tree mortality from self-thinning, wind storms, and forest management is explicitly simulated. Other
156 sources of mortality are implicitly accounted for through a so-called constant background mortality rate.
157 Furthermore, age classes (four by default) can be used after land cover change, forest management, and disturbance
158 events to explicitly simulate the regrowth of the forest. Following a land cover change, biomass and soil carbon
159 pools (but not soil water columns) are either merged or split to represent the various outcomes of a land cover
160 change. The ability of ORCHIDEE to simulate dynamic canopy structures (Naudts et al., 2015; Ryder et al., 2016;
161 Chen et al., 2016), a feature essential to simulate both the biogeochemical and biophysical effects of natural and
162 anthropogenic disturbances, is exploited in other parts of the model, i.e., precipitation interception, transpiration,
163 energy budget calculations, the radiation scheme, and the calculation of the absorbed light for photosynthesis.

164

165 Since revision 7791, mortality from bark beetle outbreaks is now explicitly accounted for and thus conceptually
166 excluded from the so-called environmental background mortality. Subsequently, changes in canopy structure
167 resulting from growth, forest management, land cover changes, wind storms, and bark beetle outbreaks are
168 accounted for in the calculations of the carbon, water, and energy exchanges between the land surface.
169 ORCHIDEE's functionality that is not of direct relevance for this study, e.g., energy budget calculations, soil
170 hydrology, snow phenology, albedo, roughness, photosynthesis, respiration, phenology, carbon and nitrogen
171 allocation, land cover changes, product use, and the nitrogen cycle are detailed in (Krinner et al., 2005; Zaehle and
172 Friend, 2010; Naudts et al., 2015; Vuichard et al., 2019).

173

174 **2.2. Origin of the bark beetle module: the LANDCLIM legacy**

175 Although mortality from windthrow (Yi-Ying et al., 2018) and forest management (Naudts et al., 2016; Luysaert et
176 al., 2018) were already accounted for in ORCHIDEE prior to r7791, insect outbreaks and their interaction with other
177 disturbances were not. The LandClim model (Schumacher, 2004) and more specifically the bark beetle module
178 developed by Temperli et al. (2013) has been used as basis to develop the bark beetle module in ORCHIDEE r7791.

179

180 LandClim is a spatially explicit stochastic landscape model in which forest dynamics are simulated at a yearly time
181 step for 10–100 km² landscapes consisting of 25 m× 25 m patches. Within a patch recruitment, growth, mortality
182 and competition among age cohorts of different tree species are simulated with a gap model (Bugmann, 1996) in
183 response to monthly mean temperature, climatic drought, and light availability. LandClim, for which a detailed

184 description can be found in (Schumacher, 2004; Temperli et al., 2013), includes the functionality to simulate the
185 decadal dynamics and consequences of bark beetle outbreaks at the landscape-scale (Temperli et al., 2013). In the
186 LandClim approach, the extent, occurrence and severity of beetle-induced tree mortality are driven by the landscape
187 susceptibility, beetle pressure, and infested tree biomass. While the LandClim beetle module was designed and
188 structured to be generally applicable for northern hemisphere climate-sensitive bark beetle-host systems, it was
189 originally parameterized to represent disturbances by the European spruce bark beetle (*Ips typographus* Linnaeus) in
190 Norway spruce (*Picea abies* Karst.; Temperli et al. 2013).

191

192 As LandClim and ORCHIDEE are developed for different purposes, their temporal and spatial scales differ. These
193 differences in model resolution justify developing a new model while still following the principles embedded in the
194 LandClim approach. LandClim assesses bark beetle damage at 25 m x 25 m patches and to do so it uses information
195 from other nearby patches as well as landscape characteristics such as slope, aspect and altitude. The susceptibility
196 of a landscape to bark beetle infestations is calculated using multiple factors such as drought-induced tree resistance,
197 age of the oldest spruce cohort, proportion of spruce in the patch's basal area, and spruce biomass damaged by
198 windthrow. These factors, presented as sigmoidal relationships, ranging from 0 to 1 (denoting none to maximum
199 susceptibility respectively) are combined in a susceptibility index for each Norway spruce cohort in a patch. Bark
200 beetle pressure is quantified as the potential number of beetles that can infest a patch, and its calculation considers,
201 among others, previous beetle activity, maximum possible spruce biomass that beetles could kill, and
202 temperature-dependent bark beetle phenology. Finally, the susceptibility index and beetle pressure are used to
203 estimate the total infested tree biomass and total biomass killed by bark beetles for each cohort within a patch.

204

205 In ORCHIDEE, however, the simulation unit is about six orders of magnitude larger, i.e. 25 km x 25 km. Hence, a
206 single pixel in ORCHIDEE exceeds the size of an entire landscape in LandClim. Where landscape characteristics in
207 LandClim can be represented by a statistical distribution, the same characteristics in ORCHIDEE are summarized in
208 a single value. These differences between LandClim and ORCHIDEE imply that the original bark beetle module
209 cannot be implemented in ORCHIDEE without deep adjustments. We develop a pixel-level model that does not
210 require spatial information and statistical distributions of landscape characteristics.

211

212 In the newly developed module of ORCHIDEE, the foundational concept is retained from LANDCLIM, yet the
213 variables influencing susceptibility calculations have largely been modified, with the exception of the phenology
214 model, which continues to follow the framework established by Temperli et al. in 2013. Given the extensive and
215 significant alterations, a direct comparison between ORCHIDEE and LANDCLIM may no longer be pertinent.
216 However, we have developed a flowchart (Fig. 2) to provide an overarching perspective of our advancements,
217 facilitating an understanding of how it diverges from the initial methodology.

218

219 **2.3. Bark beetle outbreak development stages**

220 Bark beetle outbreak development stages are useful to understand the dynamics of an outbreak (Fig. 1) and have
221 been described in numerous studies (Wermelinger, 2004; Edburg et al., 2012; Hlásny et al., 2021a). Nonetheless, in
222 ORCHIDEE r7791, we design a model framework which simulates the dynamic of bark beetle outbreak as a
223 continuous process. Hence, endemic, epidemic, build-up and post-epidemic stages are not explicitly simulated and
224 these stages were only introduced to structure the model description. If needed, these stages could be distinguished
225 while post-processing the simulation results if (arbitrary) thresholds are set for specific variables such as $i_{\text{beetles pressure}}$,
226 $i_{\text{beetles mass attack}}$, or $B_{\text{beetles kill}}$ (these variables are defined further below).
227

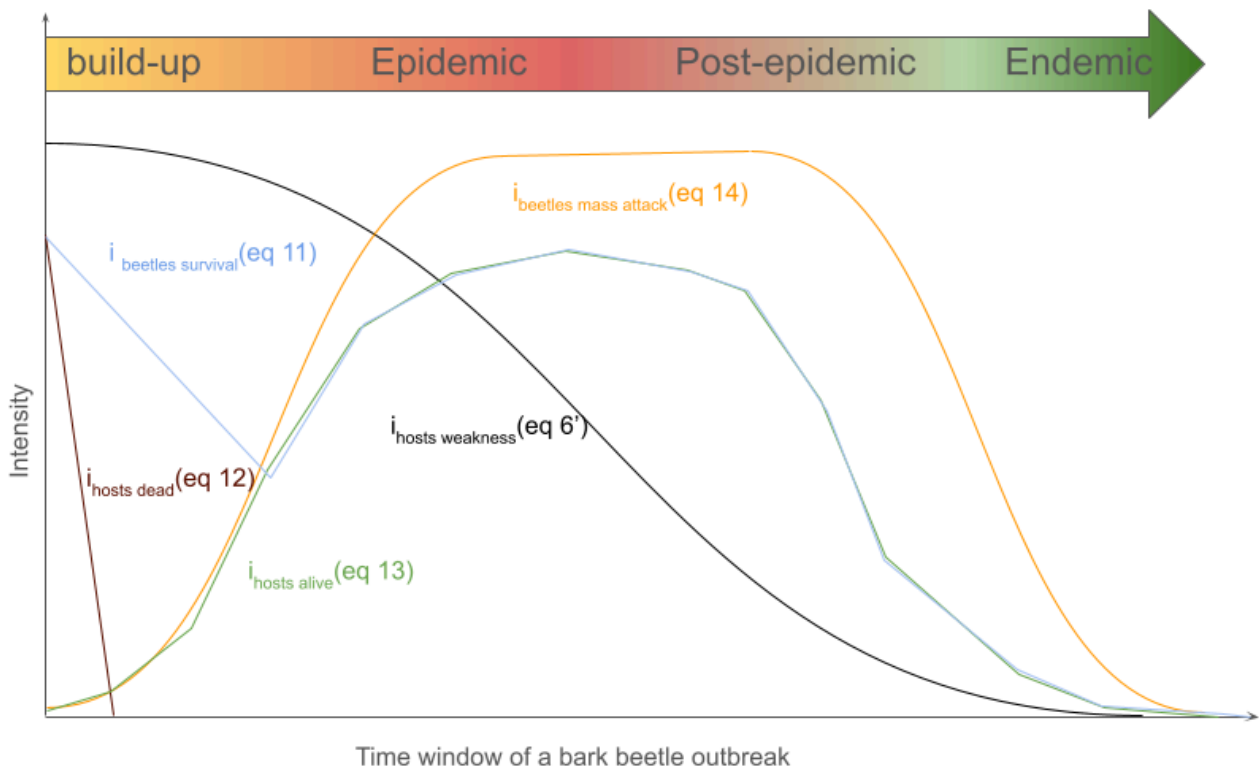


Figure 1 : This figure illustrates the dynamic interplay of factors during a bark beetle outbreak. It depicts the intensity and timeline of key variables such as beetle survival, beetles mass attack, and host weakness (section 2.4). The time window spans four outbreak development stages: build-up, epidemic, post-epidemic, and endemic. The curves represent key variables, showing the escalation of beetle attacks and subsequent decline in host population, which eventually leads to a stabilization of the system in the endemic phase.

228
 229
 230
 231
 232
 233
 234

Table 1: List of symbols

Symbol	Description	Units
α	Alpha parameter from the self thinning relationship	unitless
β	Beta parameter from the self thinning relationship	unitless
act_{limit}	B_{kill}/B_{total} at which $i_{beetles\ activity} = 0.5$	$gC.m^{-2}$
$B_{beetles\ kill}$	Biomass of spruce killed by bark beetle annually	$gC.m^{-2}$
$B_{windthrow\ kill}$	Biomass of spruce killed by windthrow event	$gC.m^{-2}$
$B_{beetles\ attacked}$	Biomass of spruce attacked by bark beetle annually	$gC.m^{-2}$
B_{total}	Total living spruce stand biomass	$gC.m^{-2}$
B_{wood}	Spruce woody biomass	$gC.m^{-2}$
BP_{limit}	$i_{beetle\ pressure}$ at which $i_{beetles\ mass\ attack} = 0.5$	unitless
D_{max}	Maximum Tree stand density	$tree.ha^{-1}$
$D_{age\ class}$	Spruce age classes stand density	$tree.ha^{-1}$
DD_{eff}	Cumulative effective Degrees Day	$^{\circ}C.Day^{-1}$
DD_{ref}	Reference Degrees Day to fulfill one beetle generation	$^{\circ}C.Day^{-1}$
$Dia_{quadratic}$	Mean quadratic diameter	meters
$DR_{beetles}$	$B_{beetles\ kill}/B_{total} * 100$	%
$DR_{windthrow}$	$B_{windthrow\ kill}/B_{total} * 100$	%
F_{spruce}	Spruce stand area fraction	unitless
$F_{age\ class}$	Spruce age classes area fraction	unitless
$F_{non-spruce}$	Non-spruce area fraction	unitless
G_{limit}	Beetles generation number at which $i_{beetle\ generation} = 0.5$	Generation
$i_{hosts_competition}$	Spruce trees under competition pressure	unitless
$i_{hosts_weakness}$	Weak to bark beetle attack spruce trees	unitless
$i_{hosts_attractivity}$	Spruce attractiveness for bark beetles	unitless
i_{hosts_dead}	defenseless spruce trees uprooted or cutted	unitless
i_{hosts_alive}	Potential living spruce hosts for bark beetle	unitless
$i_{hosts_defence}$	Spruce trees capacity to resist to a bark beetle attack	unitless
i_{hosts_share}	Spruces hidden by other species to bark beetle detection	unitless
$i_{hosts_competition, age_class}$	Weak to bark beetle attack spruce trees	unitless
$i_{hosts_defence, age\ class}$	Spruce trees capacity to resist to a bark beetle attack	unitless
$i_{hosts_health, age_class}$	Spruce trees health condition	unitless
$i_{beetles_pressure}$	Proxy of bark beetle population level	unitless
$i_{beetles_survival}$	Bark beetle winter survival index	unitless
$i_{beetles_generation}$	Bark beetle generation index	unitless
$i_{beetles_activity}$	Previous bark beetles activity index	unitless

$i_{\text{beetles_mass_attack}}$	Bark beetles mass attack capability	unitless
$\max_{N_{\text{wood}}}$	Value of N_{wood} at which $i_{\text{hosts dead}} = 1.0$	unitless
N_{wood}	Spruce wood necromass	gC.m^{-2}
$P_{\text{success, age class}}$	Probability of successful attack	unitless
P_{attack}	Probability of beetles attack	unitless
PWS_{max}	Maximum long term Spruce water stress	unitless
PWS_{spruce}	Spruce water stress	unitless
$PWS_{\text{age class}}$	Spruce age classes water stress	unitless
PWS_{limit}	Spruce water stress at which $i_{\text{hosts defense}} = 0.5$	unitless
RDi_{limit}	Relative density index at which $i_{\text{hosts competition}} = 0.5$	unitless
RDi_{weakness}	Relative density index at which $i_{\text{host weakness}} = 0.5$	unitless
RDi_{spruce}	Spruce stand relative density index [0,1]	unitless
$RDi_{\text{age class}}$	Spruce age classes relative density index [0,1]	unitless
$S_{\text{competition}}$	Shape parameter in the calculation of $i_{\text{hosts competition}}$	unitless
S_{weakness}	Shape parameter in the calculation of $i_{\text{hosts weakness}}$	unitless
S_{drought}	Shape parameter in the calculation of $i_{\text{hosts defense}}$	unitless
S_{share}	Shape parameter in the calculation of $i_{\text{hosts share}}$	unitless
S_{activity}	Shape parameter in the calculation of $i_{\text{beetle activity, y-1}}$	unitless
$S_{\text{generation}}$	Shape parameter in the calculation of $i_{\text{beetle generation}}$	unitless
Sh_{spruce}	Share fraction of Spruce	unitless
Sh_{limit}	Share fraction at which $i_{\text{hosts share}} = 0.5$	unitless
T_{air}	Air Temperature	$^{\circ}\text{C}$

236

237 The biomass of trees killed by bark beetles in one year and one pixel ($B_{\text{beetles kill}}$) is calculated as the product of the
238 biomass of trees attacked by bark beetle ($B_{\text{beetles attacked}}$) and the probability of a successful attacks ($P_{\text{success, age class}}$)
239 averaged over the number of age classes and weighted by their actual fraction ($F_{\text{age class}}$) for a given tree species
240 (F_{spruce}). The approach assumes that a successful beetle colonization always results in the death of the attacked tree
241 which is a simplification from reality (A. Leufvén et al. 1986).

242

$$243 \quad B_{\text{beetles kill}} = \sum_{\text{nb age classes}}^{age\ class=1} P_{\text{success, age class}} \times B_{\text{beetles attacked}} \times \frac{F_{\text{age class}}}{F_{\text{spruce}}} \quad (1)$$

244

245 During the endemic stage, $B_{\text{beetles attacked}}$ and $B_{\text{beetles kill}}$ are at their lowest values and the damage from bark beetles has
246 little impact on the structure and function of the forest. Losses from $B_{\text{beetles kill}}$ can be considered background
247 mortality.

248

249 The biomass of trees attacked by bark beetles ($B_{\text{beetles attacked}}$) is defined as an attempt from the bark beetles to
 250 overcome the tree defenses and thus succeeding in boring holes in the bark in order to reach the sapwood. B_{beetles}
 251 $_{\text{attacked}}$ is calculated at the pixel level by multiplying the actual stand biomass of spruce (B_{total}) and the probability that
 252 bark beetles attack spruce trees in the pixel (P_{attacked}).

253

$$254 \quad B_{\text{beetles attacked}} = B_{\text{total}} \times P_{\text{attacked}} \quad (2)$$

255

256 P_{attacked} represent the ability of the bark beetles to spread and to locate new suitable spruce trees as hosts for breeding.
 257 P_{attacked} is calculated by the product of two indexes (all indexes in this study are denoted i and are analogue the
 258 susceptibility indexes from Temperli et al. 2013): (1) the beetle pressure index ($i_{\text{beetles pressure}}$) which a proxy of the
 259 bark beetle population and (2) the stand attractiveness index ($i_{\text{hosts attractiveness}}$) which is a proxy of the overall stand
 260 health. Health was here defined as the ability of the forest to resist an external stressor such as bark beetle attacks.

261

$$262 \quad P_{\text{attacked}} = i_{\text{hosts attractiveness}} \times i_{\text{beetles pressure}} \quad (3)$$

263

264 2.5. Stand attractiveness

265 The stand attractiveness index ($i_{\text{hosts attractiveness}}$) varies between 0.5 and 1. When $i_{\text{hosts attractiveness}}$ tends to 0.5, the stand is
 266 constituted mainly by healthy trees which are less attractive for beetles whereas an $i_{\text{hosts attractiveness}}$ approaching 1
 267 represents a highly stressed forest suitable for colonization by bark beetles. Factors that contribute to the stress of a
 268 forest in ORCHIDEE are: nitrogen limitation, limited carbohydrate reserves, and monospecific spruce forest. Trees
 269 experiencing extended periods of environmental stress are expected to have less carbon and nitrogen reserves
 270 available for defense compounds, making them vulnerable for bark beetle attacks even at relatively low beetle
 271 population densities (Raffa et al., 2008). Nonetheless, reserves pools in ORCHIDEE r7791 have not yet been
 272 evaluated so, instead proxies were used such as long term drought (PWS_{max}) and relative density index (RDi) which
 273 were already simulated in ORCHIDEE r7791.

274

$$275 \quad i_{\text{hosts attractiveness}} = \max(i_{\text{hosts competition}}, i_{\text{hosts defense}}) \times i_{\text{hosts share}} \quad (4)$$

276

277 Where $i_{\text{hosts competition}}$ and $i_{\text{hosts defense}}$ both represent proxies for the reduction of the nitrogen and carbohydrate reserve
 278 due to strong competition for light and soil resources, and repetitive years that are drier than average. For this study,
 279 the average drought intensity during the last three years is considered, as a proxy of spruce stand healthiness:

280

$$281 \quad i_{\text{hosts defense}} = 1 / (1 + e^{S_{\text{drought}} \cdot (1 - PWS_{\text{max}} - PWS_{\text{limit}})}) \quad (5a)$$

282

283 Where,

284

$$PWS_{max} = \sum_{nb \text{ age class}}^{age \text{ class}=1} \max(PWS_{spruce}, \dots, PWS_{spruce, n-3}) \times \frac{F_{age \text{ class}}}{F_{spruce}} \quad (5b)$$

286

287 Where PWS_{max} is the maximum plant water stress index during the last 3 years, PWS_{limit} is the plant water stress
 288 below which the healthiness of the stand will strongly be affected. In addition to drought, overstocked forest may
 289 also decrease the overall healthiness of a spruce stand ($i_{hosts \text{ competition}}$).

290

$$i_{hosts \text{ competition}} = 1 / (1 + e^{S_{competition} \cdot (RDi_{spruce} - RDi_{limit})}) \quad (6a)$$

292

293 In ORCHIDEE, the relative density index (RDi) is used to quantify the competition between trees at the stand level.
 294 At an RDi of 1, the forest is expected to be at its maximum density given the carrying capacity of the site, implying
 295 the highest level of competition between trees. RDi_{limit} represents the limit at which the bark beetle outbreak starts to
 296 decline because of lack of suitable host trees. At the spatial scale of the ORCHIDEE model, RDi_{limit} could be
 297 considered as a parameter for spatial upscaling since it describes how many trees survive after an outbreak which is
 298 very dependent on the size of the pixel. When a pixel represents a single stand (~1 ha) all trees may be killed during
 299 an outbreak so RDi_{limit} will be setup close to 0. When an ORCHIDEE pixel is used to represent an area of 2500 km²,
 300 not all trees will be killed which is reflected in setting $RDi_{limit} = 0.4$.

301

302 RDi_{spruce} is computed as follows:

303

$$RDi_{spruce} = \sum_{nb \text{ age class}}^{age \text{ class}=1} \frac{D_{age \text{ class}}}{D_{max}} \times \frac{F_{age \text{ class}}}{F_{spruce}} \quad (6b)$$

305

306 Where $D_{age \text{ class}}$ is the current tree density of an age class and $F_{age \text{ class}}$ is the fraction of spruce in the pixel that resides
 307 in this age class. D_{max} represents the maximum stand density of a stand given its diameter. In ORCHIDEE D_{max} is
 308 calculated based on the mean quadratic diameter (cm) of the age class and two species specific parameters, α and β :

309

$$D_{max} = (Dia_{quadratic, age \text{ class}} / \alpha)^{(1/\beta)} \quad (6c)$$

311

312 The index $i_{hosts \text{ share}}$ (used in eq. 4) takes into account that in a mixed tree species landscape, even a few non-host trees
 313 may chemically hinder bark beetles in finding their host trees (Zhang and Schlyter, 2004) explaining why insect
 314 pests, including *Ips typographus* outbreaks, often cause more damage in pure compared to mixed stands (Nardi et
 315 al., 2023). ORCHIDEE r7791 does not simulate multi-species stands but does account for landscape-level
 316 heterogeneity of forests with different plant functional types. The bark beetle module in ORCHIDEE assumes that
 317 within a pixel, the fraction of spruce over other tree species is a proxy for the degree of mixture:

318

$$i_{hosts\ share} = 1 / (1 + e^{S_{share} \cdot (sh_{spruce} - sh_{limit})}) \quad (7a)$$

320

321 Where,

322

$$Sh_{spruce} = F_{none-spruce} / F_{spruce} \quad (7b)$$

324

325 2.6. Implicit representation of bark beetle populations

326 The bark beetle pressure Index ($i_{beetles\ pressure}$) is formulated based on two components: (1) the bark beetle breeding
 327 index of the current year ($i_{beetles\ generation}$), and (2) an index of the loss of tree biomass in the previous year due to bark
 328 beetle infestation ($i_{beetles\ activity}$). $i_{beetles\ activity}$ is thus a proxy of the previous year's bark beetle activity. The expression
 329 accounts for the legacy effect of bark beetle activities by averaging activities over the current and previous years. In
 330 this approach, the susceptibility index ($i_{beetles\ survival}$) serves as an indicator for increased bark beetle survival which
 331 could result from favorable conditions for beetle demography (see next section).

332

$$i_{beetles\ pressure} = i_{beetles\ survival} \times \frac{(i_{beetles\ generation} + i_{beetles\ activity})}{2} \quad (8)$$

334

335 The model calculates $i_{beetles\ generation}$ from a logistic function, which depends on the number of generations a bark
 336 beetle population can sustain within a single year:

337

$$i_{beetles\ generation} = 1 / (1 + e^{-S_{generation} \cdot (\frac{DD_{eff}}{DD_{ref}} - G_{limit})}) \quad (9)$$

339

340 Where $S_{generation}$ and G_{limit} are tuning parameters for the logistic function, DD_{eff} represents the sum of effective
 341 temperatures for bark beetle reproduction in $^{\circ}C \cdot day^{-1}$, while DD_{ref} denotes the thermal sum of degree days for
 342 one bark beetle generation in $^{\circ}C \cdot day^{-1}$. Saturation of $i_{beetles\ generation}$ represents the lack of available breeding
 343 substrate when many generations develop over a short period.

344

345 DD_{eff} is calculated from January 1st until the diapause of the first generation. In ORCHIDEE, diapause is triggered
 346 when daylength exceeds 14.5 hours (e.g., April 27th for France). Each day before the diapause with a daily average
 347 temperature above 8°C is accounted for in sumTeff. This approach simulates the phenology of bark beetles, which
 348 tend to breed earlier when winter and spring were warmer, thus allowing for multiple generations in the same year
 349 (Hlásny et al., 2021a). More details on the phenology model are available in Temperli et al. 2013.

350

351 The bark beetle activity of the previous year ($i_{beetles\ activity}$) is calculated as:

352

$$i_{\text{beetles activity}} = 1 / (1 + e^{-S_{\text{activity}} \left(\frac{B_{\text{kill}, y-1}}{B_{\text{total}}} - \text{act}_{\text{limit}} \right)}) \quad (10)$$

354

355 Where $i_{\text{beetles activity}}$ denotes the biomass of the stand damaged by bark beetles in the previous year, B_{total} is the total
 356 biomass of the stand, and S_{activity} and $\text{act}_{\text{limit}}$ are parameters that drive the intensity of this negative feedback.

357

358 During the build-up stage (Fig. 1) the population of bark beetles can either return to its endemic stage (Fig. 1) if tree
 359 defense mechanisms are preventing bark beetles from successfully attacking healthy trees, or evolve into an
 360 epidemic stage (Fig. 1) if the tree defense mechanisms fail. During this stage, tree canopies remain green, therefore,
 361 this stage is also known as the green stage (Fig. 1). During the post-epidemic stage, the forest is still subject to
 362 higher mortality than usual but signs of recovery appear (Hlásny et al., 2021a). Recovery may help the forest
 363 ecosystem to return to its original state or switch to a new state (different species, change in the forest structure)
 364 depending on the intensity and the frequency of the disturbance (Van Meerbeek et al., 2021).

365

366 2.7. Bark beetle survival

367 The capacity of the bark beetles to survive the winter in between two breeding seasons is a crucial mechanism
 368 explaining massive tree mortality due to an outbreak. During regular winters, winter mortality for bark beetles is
 369 around 40% for the adults and 100% for the juveniles (Jönsson et al. 2012). In our scheme, this mortality rate is
 370 implicitly accounted for in the calculation of the bark beetle survival index ($i_{\text{beetles survival}}$). A lack of data linking bark
 371 beetle survival to anomalous winter temperatures prevented us from including this information as a modulator of
 372 $i_{\text{beetles survival}}$. Instead the model simulates the excess of survival due to the abundance of suitable tree hosts which
 373 decreases the competition for shelter and food:

374

$$i_{\text{beetles survival}} = \max(i_{\text{hosts dead}}, i_{\text{hosts alive}}) \quad (11)$$

376

377 The availability of wood necromass from trees that died recently, particularly following windstorms, plays a critical
 378 role in bark beetle survival and proliferation. In the year following a windstorm, uprooted and broken trees may
 379 offer an ideal breeding substrate for bark beetles, facilitating their population growth.

380

381 In Temperli et al. (2013) an empirical correlation between windthrow events and bark beetle susceptibility was
 382 established. ORCHIDEE enhances realism by considering the actual suitable hosts (living or recently dead trees) as
 383 the primary driver of bark beetle survival. To avoid overestimating bark beetle population growth, \max_{Nwood} has been
 384 introduced. This ensures that an excess of breeding substrate does not artificially inflate beetle numbers,
 385 acknowledging that recent dead trees lose their freshness and thus suitability for breeding after a year. Any addition
 386 of dead trees beyond \max_{Nwood} is considered ineffective in affecting the bark beetle population.

387

388 This relationship is quantitatively represented in ORCHIDEE through the dead host index, $i_{\text{hosts dead}}$, which is driven
 389 by the availability of recent dead trees. The formulation of $i_{\text{hosts dead}}$ is as follows:

390

$$391 \ i_{\text{hosts dead}} = \min\left(\frac{N_{\text{wood}}}{B_{\text{wood}}}, \max_{N_{\text{wood}}}, 1\right) \quad (12)$$

392

393 Here, N_{wood} represents the quantity of woody necromass from the current year, B_{wood} is the total woody biomass in
 394 the stand, and $\max_{N_{\text{wood}}}$ is the threshold of the ratio $N_{\text{wood}}/B_{\text{wood}}$ signifying the maximum level. This index captures
 395 the immediate increase in dead trees post-windthrow, which may drive bark beetle breeding. However, after a year,
 396 this substrate becomes unsuitable for breeding and is excluded from the $i_{\text{hosts dead}}$ calculation.

397

398 Finally, $\max_{N_{\text{wood}}}$ can also be considered as a parameter that depends on the spatial scale of the simulation. The
 399 mortality rate of trees ($DR_{\text{windthrow}}$) that will trigger an outbreak is very different across spatial scales. Where a
 400 relatively high share of dead wood is needed to trigger an outbreak at the patch-scale, a much lower share of dead
 401 wood suffices at the landscape-scale to trigger a widespread bark beetle outbreak. So these parameters must be set
 402 up according to the spatial resolution of the simulation experiment.

403

404 $i_{\text{hosts alive}}$ denotes the survival of bark beetles which is facilitated by the abundance of suitable trees which reduces the
 405 competition among bark beetles for breeding substrates and therefore increases their survival.

406

$$407 \ i_{\text{hosts alive}} = i_{\text{beetles mass attack}} \times i_{\text{hosts weakness}} \quad (13)$$

408

409 The amount of suitable tree hosts, $i_{\text{hosts weakness}}$ is driven by two factors: (1) the abundance of weak trees which can be
 410 more easily infected by bark beetles. ORCHIDEE does not explicitly represent weak trees, but tree health is thought
 411 to decrease with an increasing density given the stand diameter. The index for host suitability is thus calculated by
 412 making use of the relative density index (RDi_{spruce}).

413

$$414 \ i_{\text{hosts weakness}} = 1 / (1 + e^{S_{\text{weakness}} \cdot (RDi_{\text{spruce}} - RDi_{\text{weakness}})}) \quad (6a')$$

415

416 Equation 6a' is close to equation 6a but the parameter S_{weakness} has been reduced by a factor of two in order to reflect
 417 that $i_{\text{hosts weakness}}$ are more sensitive to RDi than $i_{\text{hosts competition}}$. (2) $i_{\text{hosts mass attack}}$ which represent the ability of bark beetles
 418 to attack healthy trees when the number of bark beetles is large enough. This index only depends on the size of the
 419 bark beetle population ($i_{\text{beetles pressure}}$ see eq. 8)

420

$$421 \ i_{\text{hosts mass attack}} = 1 / (1 + e^{S_{\text{mass attack}} \cdot (i_{\text{beetles pressure}} - BP_{\text{limit}})}) \quad (14)$$

422

423 Where $S_{\text{hosts mass attack}}$ and BP_{limit} are parameters. $S_{\text{mass attack}}$ controls the steepness of the relationship while BP_{limit} is the
 424 bark beetle pressure index at which the population is moving from endemic to epidemic stage where mass attacks
 425 are possible.

426

427 The epidemic stage corresponds to the capability of bark beetles to mass attack healthy trees and overrule tree
 428 defenses (Biedermann et al., 2019). At this point in the outbreak, all trees are potential targets irrespective of their
 429 health. Owing to the widespread mortality of individual trees, the forest dies resulting in a stage also known as the
 430 red stage (Fig. S2, stage 3). Three causes may explain the end of an epidemic: (1) the most likely cause is a high
 431 interspecific competition among beetles for tree host when the density is decreasing (decreasing $i_{\text{hosts alive}}$) (Pineau et
 432 al., 2017; Komonen et al., 2011), (2) a series of very cold years will decrease their ability to reproduce (decreasing
 433 $i_{\text{beetles generation}}$), and (3) a rarely demonstrated increasing population of beetle predators (Berryman, 2002). In
 434 ORCHIDEE r7791, the first two causes are represented but the last, i.e., the predators are not represented.

435

436 2.8. Tree mortality from bark beetle infestation

437 When bark beetles attack a tree, the success of their attack will likely depend on the capacity of the tree to defend
 438 itself from the attack. Trees defend themselves against beetle attacks by producing secondary metabolites (Huang et
 439 al., 2020). The high carbon and nitrogen costs of these compounds limit their production to periods with
 440 environmental conditions favorable for growth (Lieutier, 2002). The probability of a successful bark beetle attack is
 441 driven by the size of the bark beetle population ($i_{\text{beetle pressure}}$) and the weakness of each tree. ORCHIDEE, however, is
 442 not simulating individual trees but rather diameter classes within an age class. An index of tree weakness for each
 443 age class ($i_{\text{hosts health, age class}}$) was calculated as:

444

$$445 P_{\text{success, age class}} = i_{\text{hosts health, age class}} \times i_{\text{beetles pressure}} \quad (15)$$

446

447 A tree rarely dies solely from bark beetle damage (except during mass attacks) as female beetles often carry
 448 blue-stain fungi, which colonizes the phloem and sapwood, blocking the water-conducting vessels of the tree. This
 449 results in tree death from carbon starvation or desiccation. As ORCHIDEE r7791 does not simulate the effects of
 450 changes in sapwood conductivity on photosynthesis and the resultant probability of tree mortality, the index of
 451 weakened trees index ($i_{\text{hosts health, age class}}$) makes use of two proxies similarly to equation 5 and 6 but simplified to be
 452 calculated only for one age class at the time:

453

$$454 i_{\text{hosts health, age class}} = \frac{(i_{\text{hosts competition, age class}} + i_{\text{hosts defense, age class}})}{2} \quad (16)$$

455

$$456 i_{\text{hosts defense, age class}} = 1 / (1 + e^{S_{\text{drought}} \cdot (1 - PWS_{\text{age class}} - PWS_{\text{limit}})}) \quad (5a')$$

457

458 Contrary to equation 5a, $PWS_{\text{age class}}$ is the plant water stress from the current year.

459

$$460 i_{\text{hosts competition, age class}} = 1 / (1 + e^{S_{\text{competition}} \cdot (RDi_{\text{age class}} - RDi_{\text{limit}})}) \quad (6a'')$$

461

$$462 RDi_{\text{age class}} = \frac{D_{\text{age class}}}{D_{\text{max}}} \quad (6b'')$$

463

464 To access the Bark beetle damage rate (DR_{beetles}), we simply divide $B_{\text{beetles kill}}$ by B_{total} .

465

466 2.9. Flow of the calculations

467 As the equations presented above contain feedback loops the flow of the calculation is shown in Fig. 2.

468

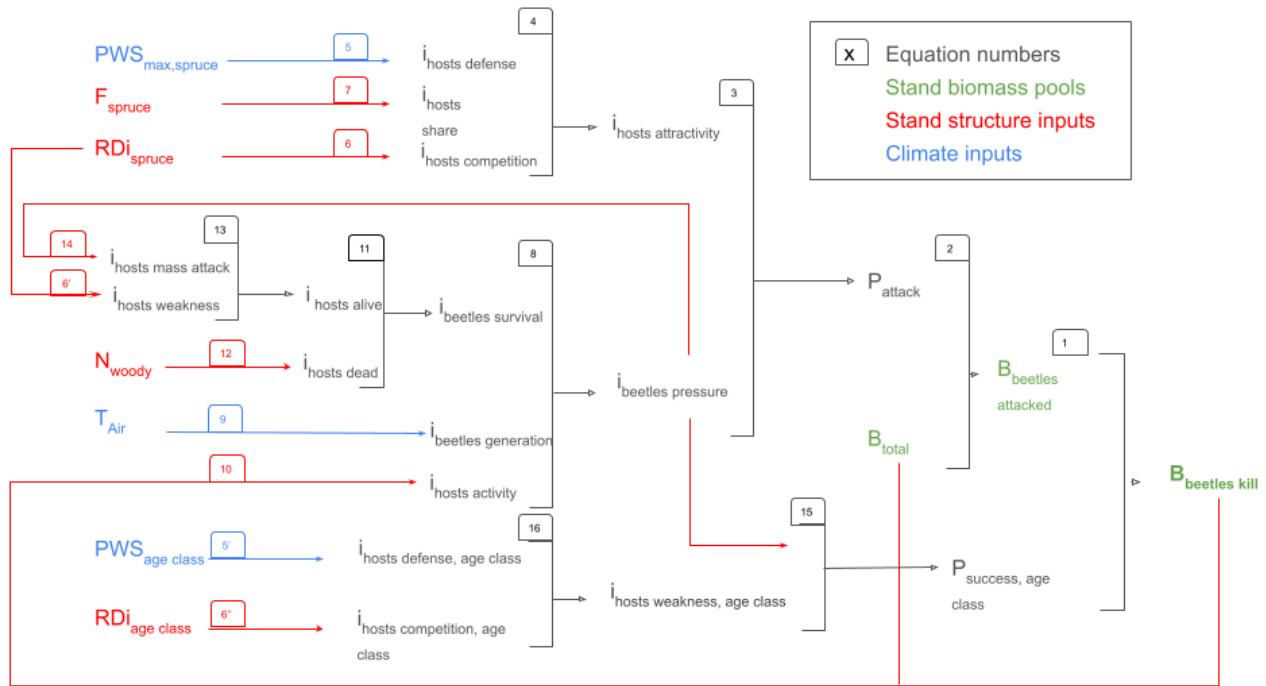


Figure 2: Flow of the calculations in the bark beetle outbreak module developed in this study. The numbers correspond to the equation numbers provided in this study.

469

470 3. Methods and material

471 3.1. Model configuration

472 Given the large-scale nature of the ORCHIDEE we carried out a sensitivity experiment of the bark beetle outbreak

473 functionality rather than focusing the evaluation on matching observed damage volumes at specific case studies.

474 Such an approach is thought to reduce the risk of overfitting the model to specific site conditions (Abramowitz et al.,

475 2008).

476

477 ORCHIDEE r7791 including the bark beetle module was run for 8 FLUXNET sites, selected to simulate a credible
478 temperature and precipitation gradient for spruce (see further below). For each location, the half-hourly
479 meteorological data from the flux tower were gap filled and reformatted so that they could be used as climate
480 forcing by the ORCHIDEE. Boundary conditions for ORCHIDEE, such as soil texture, pH and soil color were
481 retrieved from the USDA map, for the corresponding pixel. The observed land cover and land use for the pixel were
482 ignored and set to pure spruce because this study did not investigate the effect of species mixture in the simulation
483 experiments. The resolution of the pixel chosen for this analysis is 2500 km². It corresponds to a fine resolution for
484 ORCHIDEE large-scale simulations but a coarse resolution for studying bark beetle outbreaks.

485

486 The climate forcings were looped over as much as needed to bring the carbon, nitrogen, and water pools to
487 equilibrium during a 340 years long spinup followed by a windthrow event and a 100-years simulation. The results
488 presented in this study come from the 100-years long site simulations. Given the focus on even-aged monospecific
489 spruce forests in regions where spruce growth is not constrained by precipitation, variables such as $i_{\text{hosts share}}$ and i_{hosts}
490 _{defense} were omitted from this study. Note that ORCHIDEE do not account for possible acclimation of the bark beetle
491 population to each location.

492

493 3.2. Site selection

494 Bark beetle populations are known to be sensitive to temperature as they are more likely to survive a mild winter
495 (Lombardero et al., 2000) and tend to breed earlier when winter and spring are warmer than usual, allowing for
496 multiple generations in the same year (Hlásny et al., 2021a). In order to assess the temperature effect of the bark
497 beetle outbreak module in ORCHIDEE, eight locations in Europe were selected (Table 2) which represent the range
498 of climatic conditions within the distribution area of Norway spruce (*Picea Abies* Karst L.) which is the main host
499 plant for *Ips typographus*, the bark beetle species under investigation.

500

501 **Table 2: Climate characteristics of the eight sites used in the simulation experiments gradient underlying our**
experimental setup. The site acronyms refer to the site names used in the FLUXNET database (Pastorello et al.
2020).

Site (FLUXNET)	HYY	SOR	THA	WET	HES	FON	REN	COL
Full name	Hyttiala	Soroe	Tharandt	Wetstein	Hesse	Fontainebleau	Renon	Collelongo
Country	Finland	Danmark	Germany	Germany	France	France	Italy	Italy
Latitude (°N)	61.8	55.5	50.9	49.0	48.4	48.7	46.5	41.8
Longitude (°E)	24.3	11.6	13.6	14.8	7.1	2.8	11.4	13.6
MAT (°C)	3.8	8.2	8.2	7.7	9.5	10.2	4.7	6.3
MinAT (°C)	-10.8	2.7	-3.9	-5.2	0.1	-1.1	-6.3	-3.8
MAP (mm.y ⁻¹)	522	811	734	587	653	989	752	1050
Mean annual net radiation (w.m ⁻²)	42.1	49.4	52.5	68.0	53.7	50.3	67.7	68.3

502 For these eight locations, half-hourly weather data from the FLUXNET database (Pastorello et al., 2020) were used
503 to drive ORCHIDEE. Some of these locations (FON, SOR, HES, COL, WET) are in reality not covered by spruce
504 but all sites are, however, located within the distribution of Norway spruce. In this study, site locations were selected
505 to use observed weather data to simulate a credible temperature and rainfall gradient for spruce.

506

507 3.3. Sensitivity to model parameters

508 The sensitivity assessment evaluates the responsiveness of four key variables ($i_{\text{hosts weakness}}$, $i_{\text{beetles mass attack}}$, $i_{\text{beetles generation}}$,
509 $i_{\text{beetles activity}}$) of the bark beetle model of ORCHIDEE. The assessment aims to demonstrate the ability of ORCHIDEE
510 to simulate diverse dynamics of bark beetle infestations. The selection of $i_{\text{hosts weakness}}$, $i_{\text{beetles activity}}$, $i_{\text{beetles mass attack}}$, and
511 $i_{\text{beetles generation}}$ was based on two criteria: (1) their substantial influence on the dynamics of the bark beetle epidemic,
512 and (2) their independence from direct measurable data, rendering them less suitable for evaluation through
513 literature review.

514

515 For each variable, three distinct values were assigned to two parameters labeled “S” and “limit”. The S parameter
516 determines the shape of the logistic relationship, with three values tested for each variable: (a) $S=-1$, yielding a
517 linear relationship, (b) $-1 < S < -100$, resulting in a logistic curve, and (c) $S > -100$, turning the logistic relationship into
518 a step function.

519

520 The second parameter called “Limit” determines the threshold, derived from expert insights, at which the logistic
521 relationship will reach its midpoint value of 0.5 (RDI_{weakness} , BP_{limit} , Act_{limit} or G_{limit}). For instance, RDI_{weakness} is set at
522 0.55, indicating $i_{\text{hosts weaknes}}$ midpoint sensitivity (Eq. 6’). Setting BP_{limit} at 0.12 results in an $i_{\text{beetles mass attack}}$ midpoint
523 when $i_{\text{beetles pressure}}$ is 0.12, selected for its proximity to scenarios where $i_{\text{hosts dead}}$ equals 1.0 (Eq. 14). Act_{limit} was
524 positioned at 0.06, signifies $i_{\text{beetles activity}}$ midpoint at a $DR_{\text{beetles}} = 6\%$ from the preceding year, exceeding endemic
525 levels yet not reaching epidemic outbreaks (Eq. 10). Lastly, G_{limit} is fixed at 1.0, denoting $i_{\text{beetles generation}}$ ’s midpoint
526 upon completing one generation annually, underpinning the rarity of bark beetle outbreaks with fewer than one
527 generation per year (Eq. 9). Starting from these reference values, a “restrictive” simulation was run in which the
528 “Limit” parameter values were reduced by 50%. Likewise a “permissive” simulation was run to test 50% higher
529 “Limit” parameter values.

530

531 This assessment explores 36 parameters value combinations (3 x 3 parameter values x 4 parameters). The
532 simulations were run for the THA site, where they were repeated for a $DR_{\text{windthrow}}$ of 0.1 and 10%. The effect of the
533 parameters with a negligible windthrow event, i.e., killing only 0.1% of the trees, was tested to confirm that the
534 selected parameters did not simulate false positives, i.e. ORCHIDEE simulating a bark beetle outbreak in the
535 absence of windthrow. Note that this sensitivity analysis aims to document model behavior, rather than seeking
536 precise parameter values (see section 3.4).

537

538 3.4. Parameter tuning

539 The simulation experiment presented in this section was repeated for all eight sites and those results were used to
540 tune key model parameters. In order to select parameters values for $i_{\text{hosts weaknes}}$, $i_{\text{beetles mass attack}}$, $i_{\text{beetles generation}}$, $i_{\text{beetles activity}}$
541 that resulted in simulations reproducing observed dynamics of bark beetle outbreaks, the literature was searched for
542 peer-reviewed papers that reported quantitative characteristics of bark beetle outbreaks (Table 3). Four
543 characteristics could be documented:

- 544 ● The delay between the windthrow event and the start of the bark beetle outbreak.
- 545 ● The length of the bark beetle outbreak is defined by the number of years required for a bark beetle
546 population to go back to its endemic level.
- 547 ● The cumulative number of trees per unit area, killed by the bark beetles at the end of an outbreak.
- 548 ● The tree mortality rate (DR_{beetles}) during an endemic stage.

549

550 As already mentioned in the section 2.4, at landscapes scale we do not expect that the all spruces in the landscape
551 will be killed by an outbreak, so we choose to set RDI_{limit} to 0.4 which mean that an outbreak will not kill more than
552 60 % of the trees in one pixel irrespective of the outbreak intensity.

Table 3 : Literature-based summary of characteristics of large-scale bark beetle outbreaks.

Outbreak characteristics	Observations/model outputs from literatures	How to check in ORCHIDEE ?
Delay before the start of an outbreak	A notable surge in the population of <i>I. typographus</i> , a species of bark beetle, was observed in windthrow areas during the second to third summer following the storm (Wichmann and Ravn, 2001; Wermelinger, 2004; Kärvelo and Schroeder, 2010; Havašová et al., 2017).	Using the tree mortality rate by bark beetles ($DR_{beetles}$), one can measure the number of years since the storm before reaching the maximum mortality rate (epidemic stage).
Length of an outbreak	Studies suggest that bark beetle outbreaks in Europe can last anywhere from 11 to 17 years (Hlásny et al., 2021b; Mezei et al., 2014; Bakke, 1989).	Using the tree mortality rate by bark beetles ($DR_{beetles}$), one can measure the number of years since the storm before reaching the minimum mortality rate (endemic stage).
Severity rate of an outbreak	A severe bark beetle outbreak resulted in a 52%-60% reduction in tree numbers at large landscape scale (>2000km ²) (Pfeifer et al., 2011; Morehouse et al., 2008)	Count the number of trees killed by bark beetles until the end of the outbreak, then divide by the number of trees just after the storm event.
Endemic mortality rate	Total background mortality is around 1.2%/year. Bark beetles are estimated to account for 40% of the total mortality ($\approx 0.5\%/year$) (Das et al., 2016; Berner et al., 2017; Hlásny et al., 2021b).	After the end of the outbreak, count the number of trees that die every year. Then average it.

553

554 **3.5. Impact of climate and windthrow : simulation experiment**

555 In this simulation experiment, the amount of fresh dead tree hosts (N_{wood}) used by the bark beetles to breed was
556 controlled by modifying the maximum damage rate of a windthrow event ($DR_{windthrow}$) in ORCHIDEE. Seven
557 $DR_{windthrow}$ were simulated (i.e. 0.1%, 5%, 7.5%, 10%, 15%, 20%, 35%). Given the monotonic nature of the
558 relationships between $DR_{windthrow}$ and $i_{hosts\ dead}$ (Eq. 12), each event triggers a proportional increase in the dead host
559 availability ($i_{hosts\ dead}$) scaling between 0 and 1 (Fig. 3). Through its equations, ORCHIDEE assumes that for damage
560 rates above 20% $i_{hosts\ dead}$ will always be equal to 1.0. RDi_{spruce} , however, may further decrease with increasing
561 windthrow damage, which makes the 35% damage rate still interesting to investigate. Although the simulations were
562 run for all $DR_{windthrow}$, only four windthrow damage rates were presented to enhance the readability of the result
563 section including a windstorm resulting in a 35% damage rate (Fig. 3).

564

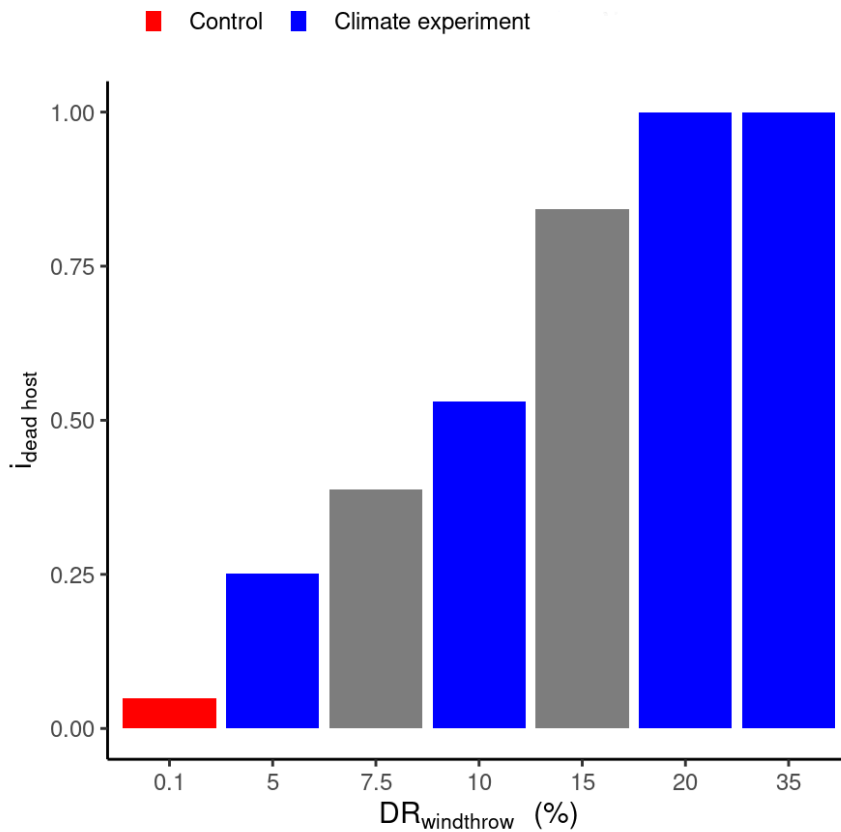


Figure 3: Relationship between windthrow damage rate ($DR_{windthrow}$) and dead host index ($i_{hosts\ dead}$). For each site a $DR_{windthrow}=0.1\%$ was used as the control simulation because an endemic bark beetle population is expected following such a low intensity event. Four $DR_{windthrow}$ were selected for subsequent presentation of the results because they cover the entire range for the $i_{hosts\ dead}$.

565

566 Site selection was based on the average numbers of generation a bark beetle population can achieve in one year. As
 567 described in Temperli 2013, the main driver of numbers of generation a bark beetle population can achieve in one
 568 year is the number of days higher than 7.5°C during winter time which is the reason why temperature is so important
 569 for bark beetle reproduction. By taking REN, THA, WET and HES, we can investigate a range in bark beetle
 570 generations between 0.8 and 3.5 (Fig. 3) which is a relevant range already observed in Europe. Restraining our
 571 analysis to only four sites will simplify the presentation in the results section.

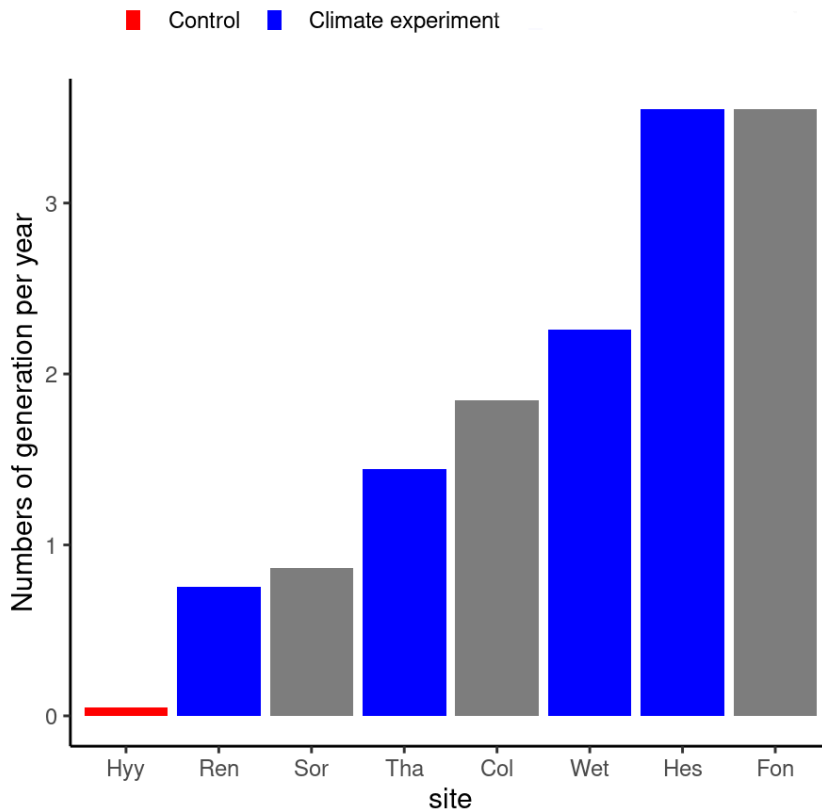


Figure 4: Average number of bark beetle generations during the 5 years following the wind storm for the 8 sites. The HYY site in Finland was selected as the control site for the REN, THA, WET and HES sites. Only results from the control and selected sites are shown in the results to enhance readability of the figures. Although all simulations were also run for SOR, COL and FON their results were found to be too similar to the results of selected sites to present them as well.

572

573 For the climate gradient, the HYY site was chosen to serve as a control since the numbers of generation is lower
 574 than 1 for which no outbreak should happen under any circumstances. Under present climate conditions, an outbreak
 575 in HYY should be considered as a false positive. Likewise, a $DR_{windthrow}=0.1\%$ is considered too low to trigger an
 576 outbreak and was therefore used as the control for the wind damage rate tests.

577

578 The experiment consisted of 25 simulations, i.e., 5 selected sites (including a control) x 5 wind damage rates
 579 (including a control). Three output variables were assessed: bark beetle damage rate ($DR_{beetles}$), total biomass (B_{total}),
 580 and net primary production (NPP). Total was investigated over 100 years whereas $DR_{beetles}$ and NPP were assessed
 581 for the first 20 years following a windthrow.

582

583

3.6. Continuous vs abrupt mortality

584 Where most land surface models use a turnover time to simulate continuous mortality (Turner et al., 2017; Pugh et
585 al., 2017), ecological reality is better described by abrupt mortality events. An idealized simulation experiment was
586 used to qualify the impact of abrupt mortality on net biome productivity by changing from a framework in which
587 mortality is approximated by a constant background mortality to a framework in which mortality occurs in abrupt,
588 discrete events. To test the impact of a change in mortality framework two versions of ORCHIDEE were compared
589 to create an idealized simulation experiment: (1) a version simulating mortality as a continuous process, labeled
590 "the smooth version", and (2) the version capable of simulating abrupt mortality from windthrow and subsequent
591 bark beetle outbreaks, labeled "the abrupt version" and (3) a version in which windthrow is activated but bark
592 beetles outbreak is include in the mortality background. The effect of simulating abrupt mortality was evaluated over
593 20, 50, and 100 year time horizons.

594

595 The effect of changing the framework of simulating mortality from continuous to abrupt was qualified on the basis
596 of 120 simulations (8 sites x 7 windthrow damage rates x 2 model versions + 8 x 1 smooth version) of 100 years
597 each. The simulations with abrupt mortality were run first. Subsequently, the number of trees killed was quantified
598 and used as a reference value for the continuous mortality set-up. This approach resulted in the same quantities of
599 dead trees at the end of the simulation for both frameworks, which then differed only in the timing of the simulated
600 mortality. This precaution is necessary to avoid comparing two different mortality regimes where the result would
601 mainly be explained by the intensity of the mortality rather than by its underlying mechanisms.

602

603 Changes in forest functioning were evaluated through the temporal evolution of accumulated net biome productivity
604 (NBP) over a 100-years time frame. NBP is defined as the regional net carbon accumulation after considering losses
605 of carbon from fire, harvest, and other episodic disturbances. NBP is a key variable in the carbon cycle of forest
606 ecosystems) as it integrates photosynthesis, autotrophic, and heterotrophic respiration. In ORCHIDEE, NBP is
607 calculated as proposed in Chapin et al., 2006). Changes in net biome productivity are thus the result of changes in
608 photosynthesis, which in turn is driven by changes in leaf area, autotrophic respiration, and heterotrophic respiration.
609 The latter is influenced by the availability of litter inputs, including litter from trees that died from the bark beetle
610 outbreak.

611

612 4. Results

613 4.1. Sensitivity to model parameters

614 The impact of spruce stand competition ($i_{\text{hosts weakness}}$) on outbreak dynamics was examined by adjusting the
615 parameters S_{weakness} and RDi_{weakness} in equation 6a'. When S_{weakness} resulted in a linear relationship ($S_{\text{weakness}} = -1$), no
616 peak in bark beetle damage occurred for the three tested values of RDi_{weakness} (permissive, reference, restrictive) at a
617 10% windthrow damage rate (Fig. 5, 4th row, 2nd column). However, employing a step function ($S_{\text{weakness}} > -100$) led
618 to either sporadic peaks of bark beetle damage with a permissive RDi_{weakness} or a two-year outbreak with a maximum
619 damage rate of 60% with a restrictive RDi_{weakness} (Fig. 5, 4th row, 2nd column), neither of which aligns with the
620 observations summarized in Table 3.

621

622 The most favorable outcome was obtained with a logistic relationship ($-1 < S_{\text{weakness}} \ll -100$), where RDi_{weakness}
623 dictated the duration of the outbreak: 11, 16, and 25 years for restrictive, reference, and permissive parameter values,
624 respectively (Fig. 5, 4th row, 2nd column). Either the restrictive or reference parameter value could be utilized since a
625 range of 11-16 years aligns with the observations (Table 3). To examine false positives, sensitivity tests were
626 repeated for a 0.1% windthrow damage rate. None of the nine parameter combinations triggered an outbreak (Fig. 5,
627 4th row, 1st column), suggesting that false positives due to the calculation of $i_{\text{hosts weakness}}$ are improbable.

628

629 The feedback effect of bark beetle mass attack capability ($i_{\text{beetles mass attack}}$) when the bark beetle population reaches a
630 certain threshold was evaluated by varying $S_{\text{mass attack}}$ and BP_{limit} (Eq. 14). Linear relationships ($S_{\text{mass attack}} = -1$) resulted
631 in similar outbreak dynamics for all BP_{limit} values, with the model settling on a constant endemic damage
632 post-outbreak, though higher than observed (Table 3). Introducing a logistic or step function minimally altered
633 outbreak dynamics except when assuming a step function for the restrictive value, which prevented an
634 outbreak. Repeating sensitivity tests for a 0.1% windthrow damage rate showed that assuming linear or logistic
635 relationships could trigger an outbreak (Fig. 5, 3th row, 1st column), indicating that false positives may arise from the
636 calculation of $i_{\text{hosts mass attack}}$.

637

638 The impact of bark beetle activities from the previous year ($i_{\text{beetles activity}}$) on outbreak dynamics was investigated by
639 varying S_{activity} and act_{limit} (Eq. 10). Linear or logistic relationships resulted in overly prolonged outbreaks (>30 years)
640 compared to observations (Table 3, 1st row, 2nd column), whereas assuming a step-function relationship simulated a
641 decline in the outbreak after 14 years. Sensitivity tests repeated for a 0.1% windthrow damage rate showed that
642 assuming a linear relationship could trigger an outbreak (Fig. 5, 1st row, 1st column), suggesting potential false
643 positives from the calculation of $i_{\text{beetles activity}}$.

644

645 To explore the effect of bark beetle activities from the previous year on outbreak dynamics ($i_{\text{hosts generation}}$), $S_{\text{generation}}$ and
646 G_{limit} from equation 9 were varied. Bark beetle damage rate was more sensitive to G_{limit} than $S_{\text{generation}}$, but only a linear
647 relationship with the reference $G_{\text{limit}} = 1.0$ yielded an intermediate outbreak intensity consistent with the location
648 (continental climate). Other combinations resulted in either too strong or no peak during the outbreak. Repeating
649 sensitivity tests for a 0.1% windthrow damage rate showed that none of the nine parameter combinations triggered
650 an outbreak (Fig. 5 2nd row, 1st column), indicating that false positives from the calculation of $i_{\text{beetles generation}}$ are
651 unlikely.

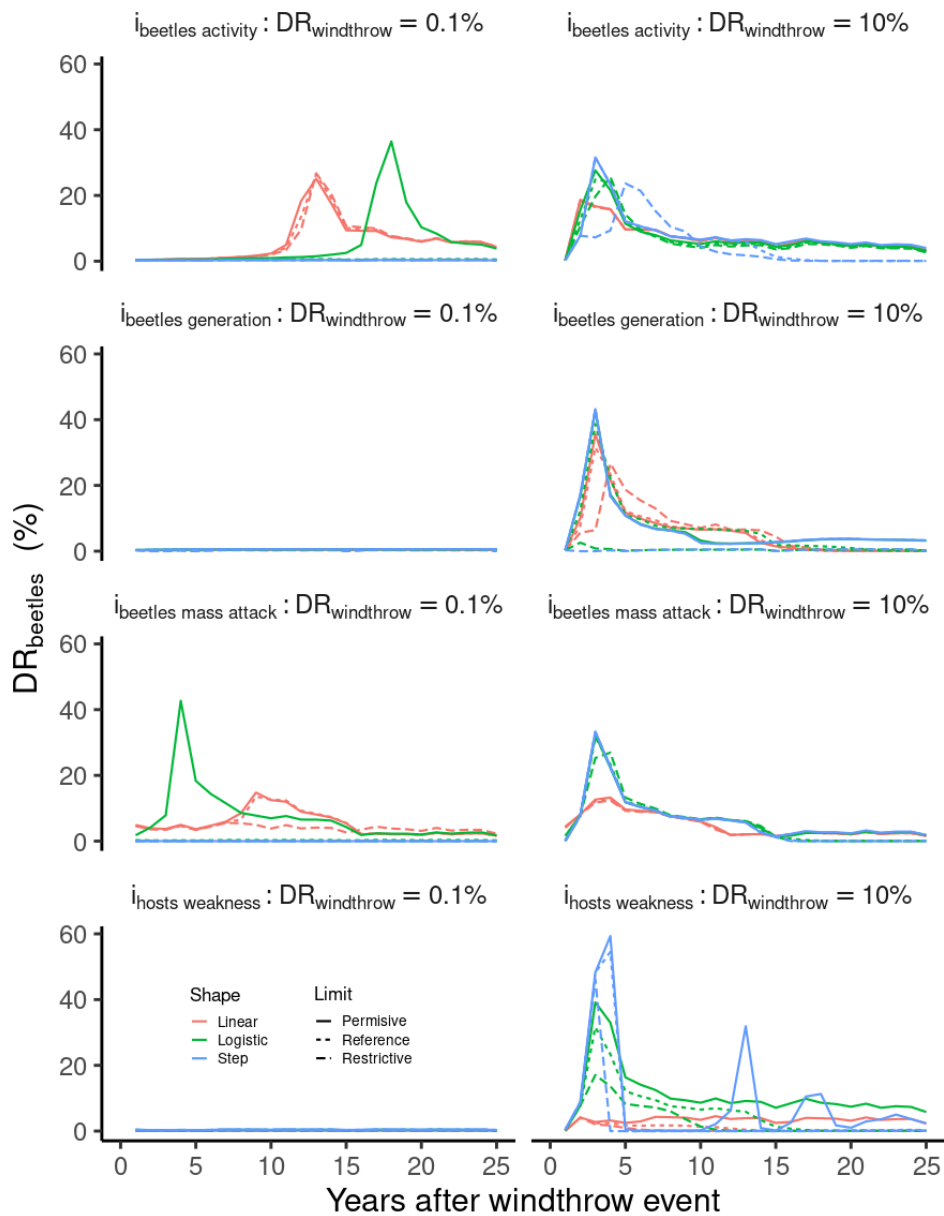


Figure 5: Simulation results from the sensitivity experiment at the THA site. Eight parameters from four equations were evaluated. Each equation represents an index from the bark beetle outbreak module ($i_{\text{hosts weakness}}$, $i_{\text{hosts mass attack}}$, $i_{\text{beetles activity}}$, $i_{\text{beetles generation}}$). Each index is represented by a logistic function defined by a shape parameter (S) and a limit parameter (L). Three values were chosen for each parameter resulting in 9 pairs of parameters for each index. Colored lines represent the shape parameter varying from linear : $S = -1$, logistic $-1 < S < -100$, to step function where $S < -100$. Line type represents three different values for L parameters where references are values of $RD_{i_{\text{weakness}}}$, $BP_{i_{\text{limit}}}$, $act_{i_{\text{limit}}}$ and $G_{i_{\text{limit}}}$ (given in Table 4), whereas permissive and restrictive represent a 50% decrease or increase respectively.

652

653

4.2. Model tuning

654 By comparing the outcomes of the sensitivity tests (section 4.1) to a summary of observations (Table 3), a first
655 estimate of the values of several parameters was proposed (Table 4).

Table 4: Parameters values from the bark beetle module tested in the sensitivity analysis. Values labeled with (*) correspond to the parameters adjusted following the sensitivity analysis results.

Parameter	Source	Value
$S_{\text{generation}}$	This study: from SA (see 3.1.4)	-1.0 (*)
G_{limit}	Adapted from Temperli et al. 2013	1.0 (*)
DD_{ref}	Adapted from Temperli et al. 2013	547.0
S_{drought}	Adapted from Temperli et al. 2013	-9.5
PWS_{limit}	Adapted from Temperli et al. 2013	0.4
$\max_{N_{\text{wood}}}$	This study: scale dependent (see 2.4.2)	0.2
S_{activity}	This study: from SA (see 3.1.3)	-500 (*)
act_{limit}	This study: from SA (see 3.1.3)	0.06 (*)
S_{weakness}	This study: from SA (see 3.1.1)	-5.0 (*)
RDi_{weakness}	This study: from SA (see 3.1.1)	0.55 (*)
RDi_{limit}	This study: scale dependent (see 2.4.1)	0.4
$S_{\text{mass attack}}$	This study: From SA (see 3.1.2)	-30.0 (*)
BP_{limit}	This study: scale dependent (see 3.1.2)	0.12 (*)
S_{share}	This study: not used (see 2.5)	15.5
SH_{limit}	This study: not used (see 2.5)	0.6

656

657

4.3. Impact of climate and windthrow on bark beetle damage

658 In ORCHIDEE, the hottest sites, HES and WET, experienced significant bark beetle outbreaks across a wide
659 spectrum of windthrow mortality rates, whereas colder sites like REN and THA saw outbreaks only in response to
660 the most severe windthrow events (Fig. 6). A greater average number of bark beetle generations in the years
661 following windthrow events led to higher bark beetle damage rates at the peak of outbreaks. For instance, at a 35%
662 windthrow mortality rate, HES reached a maximum bark beetle damage rate of 50%, whereas REN's maximum was
663 22% (Fig. 6).

664

665 Interestingly, high windthrow mortality rates could also lead to delays and lower maximum DR_{beetles} (Fig. 6). For
666 instance, at the HES site, 10%, 20%, and 35% windthrow damage rates triggered maximum DR_{beetles} of 50%, 43%,
667 and 37%, respectively (Fig. 6). Conversely, low $DR_{\text{windthrow}}$, like 5% at WET, delayed the peak of bark beetle

668 outbreaks by 9 years (Fig. 6). Additionally, the model simulated a post-epidemic stage during which the outbreak
 669 damage rate remained relatively low (<10%) and lasted between 3 to 10 years (Fig. 6). Overall, the simulated
 670 outbreaks lasted between 11 to 20 years, consistent with field observations (Table 3).

671

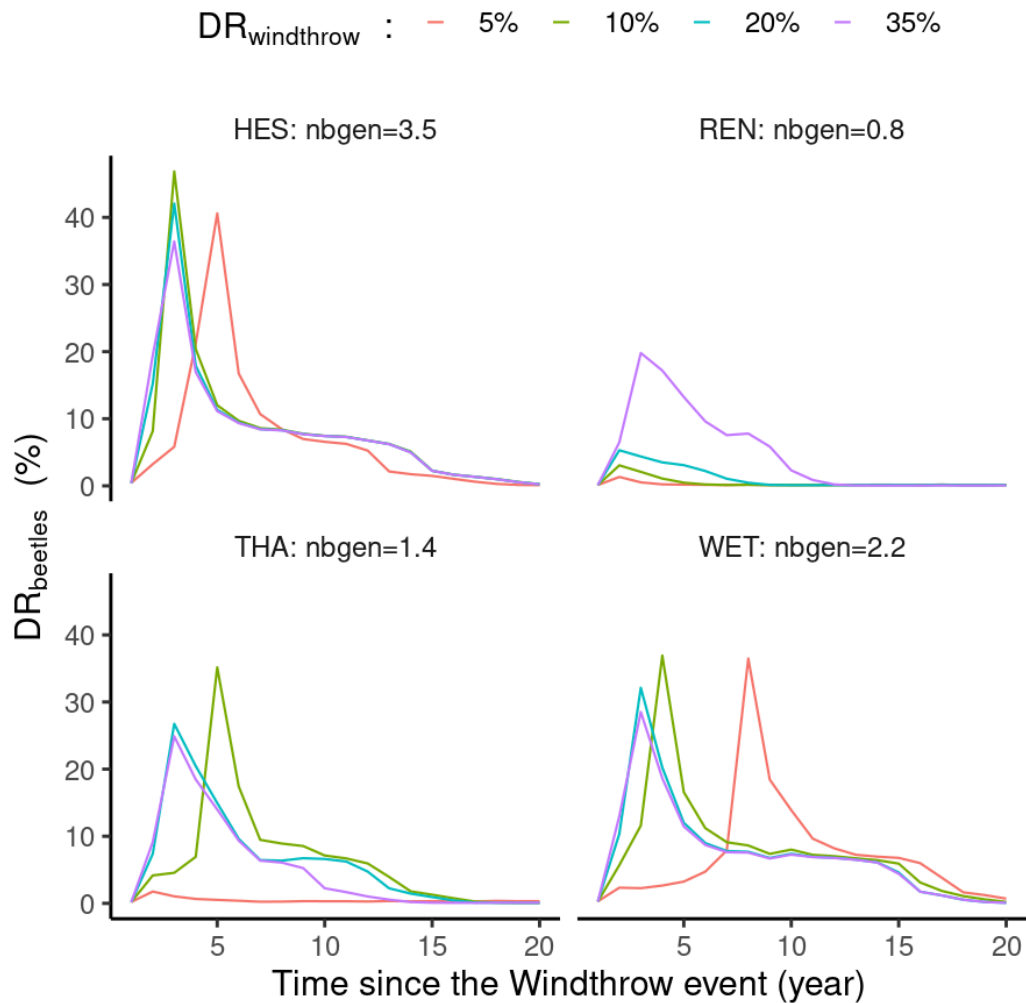


Figure 6: Simulation results of 24 simulations (4 sites x 4 windthrow damage rate $DR_{windthrow}$). Lines represent the annual bark beetle damage rate as a fraction of the total biomass ($DR_{beetles}$). Nbgen is the average number of bark beetle generations during five years after the windthrow event. $DR_{windthrow}$ represents the percentage of biomass loss by a windthrow event at the start of the simulation.

672

673 At the coldest site, HYY, ORCHIDEE predicted only a small number of bark beetle generations, preventing
 674 outbreaks from occurring. This observation validates the initial parameter tuning (Table 4), indicating that it is
 675 robust enough to prevent false positives, such as the model triggering outbreaks in sites where bark beetles cannot
 676 reproduce.

677

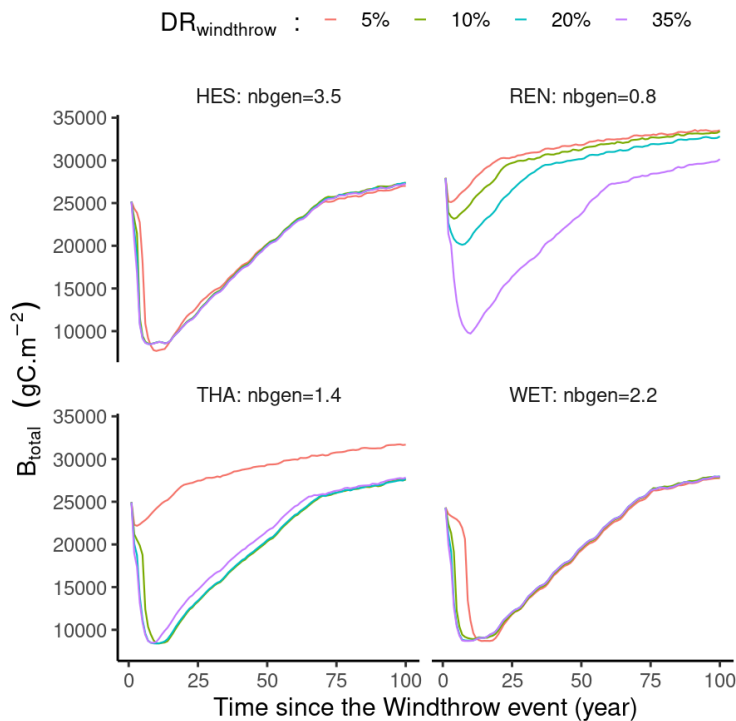
4.4. Impact of climate and windthrow on stand biomass and Net Primary Production

678 With the exception of REN, all sites experience a decrease in total biomass until around 9.000 gC.m⁻² by the end of
679 the outbreak, which typically lasted 10 to 20 years (Fig. 7). It is noteworthy that regardless of the severity of
680 maximum damage inflicted by bark beetles, the overall cumulative damage consistently results in the same amount
681 of biomass loss (Fig. 7). This characteristic is a key objective of the bark beetle module. Essentially, the model can
682 simulate significant epidemic events even if the initial trigger, such as the windthrow event in our study, is not
683 particularly intense. Once a tipping point is reached, at a biomass level of 9.000 gC.m⁻² or $R_{Di_{limit}} = 0.4$, there's no
684 turning back until that threshold is passed. Interestingly, at the REN site where the number of generations is is
685 approximately one, the outbreak only reaches the tipping point with a high windthrow damage rate (35%) (Fig. 7).

686

687 Throughout the outbreak period, there was a notable decrease in Net Primary Productivity (NPP), as illustrated in
688 the second panel in Fig. 7, primarily attributed to a sharp decline in leaf area index, although not explicitly depicted.
689 Subsequent to the epidemic phase, the forest undergoes recovery by regenerating its leaf area index. Consequently,
690 individual leaf area indices tend to escalate to attain the overall stand leaf area index, concurrently boosting
691 individual growth rates. Following the outbreak, the reduction in stand tree density due to bark beetle damage
692 mitigates autotrophic respiration, albeit not displayed, and fosters recruitment, also not depicted, thereby augmenting
693 NPP or forest growth (Fig. 7). Consequently, carbon use efficiency tends to be higher in sparsely populated stands
694 compared to densely populated ones.

695



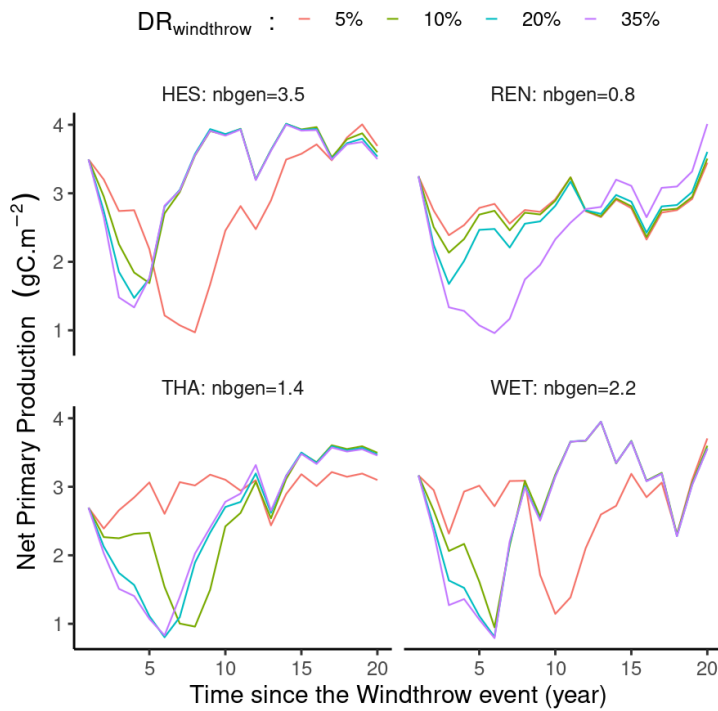


Figure 7: Simulation results of 24 simulations (4 sites x 4 windthrow mortality rate). Lines represent the annual average net primary production (NPP) in $\text{gC}\cdot\text{m}^{-2}$ or Total stand biomass (B_{total}) in $\text{gC}\cdot\text{m}^{-2}$. Nbgen is the average number of achieved bark beetle generations during five years after the windthrow event. $DR_{\text{windthrow}}$ represents the percentage of biomass loss by a windthrow event at the start of the simulation.

696

697

4.5. Continuous vs abrupt mortality

698

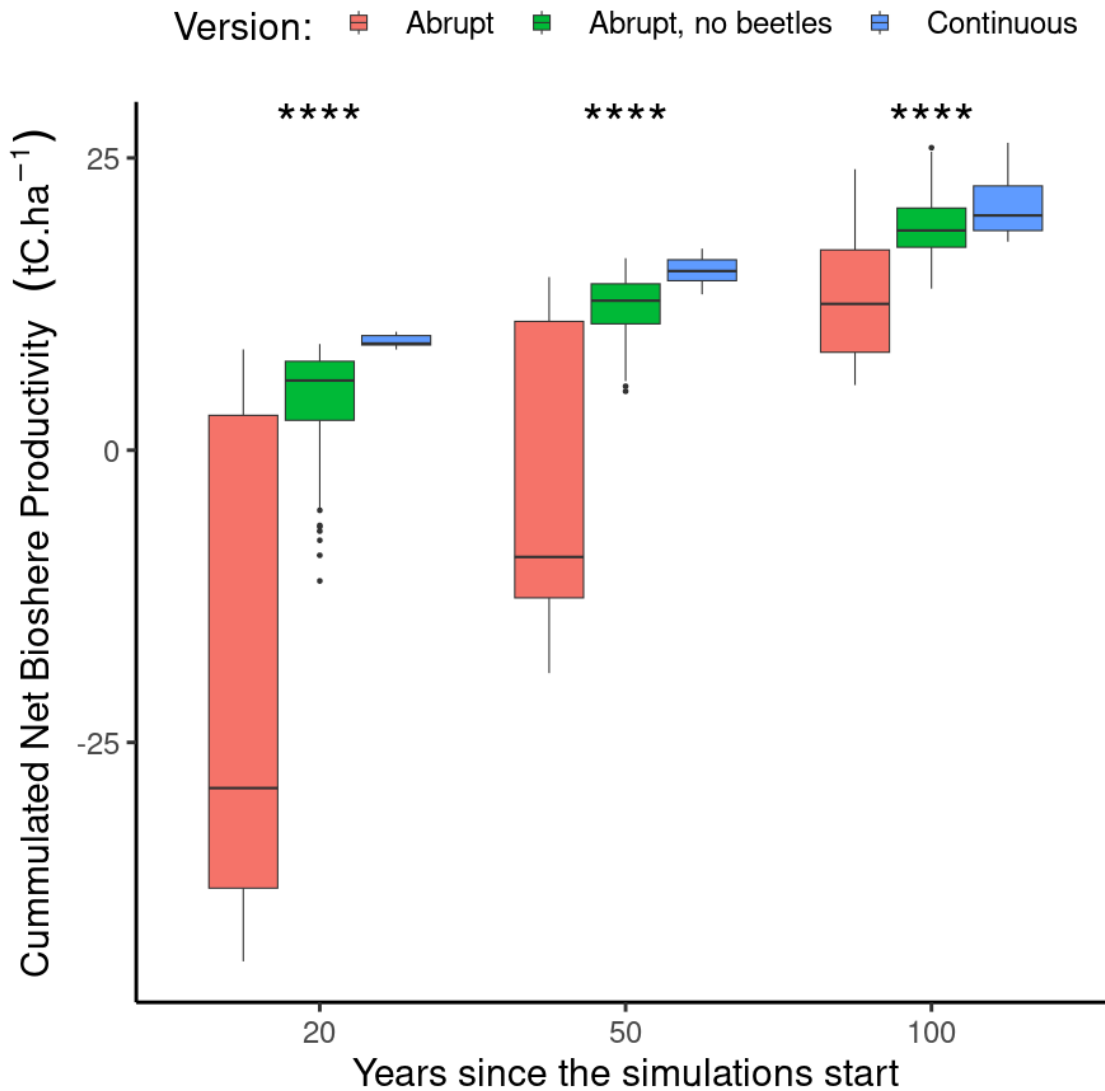


Figure 8: Difference in cumulative net biome production at three discrete time horizons (i.e. 20, 50 and 100 years) between a continuous (blue, n=8), abrupt (red, n=56), abrupt with no bark beetles outbreak (green, n=56) mortality framework. Note that in the continuous mortality framework the mortality rate was adjusted to obtain a similar number of trees killed after 100 years as in the abrupt mortality framework. The variation of each boxplot arises due to different locations and prescribed storm intensities. Each boxplot displays the median value (thick horizontal line), the quartile range (box border), and the 95% confidence interval (vertical line).

699 The total accumulated net biome production (NBP) was evaluated using the ORCHIDEE model across three
 700 different timeframes: 20, 50, and 100 years. At the 20-years mark, the average accumulated NBP notably differed
 701 between the continuous, abrupt and the abrupt without bark beetles outbreak (abrupt, no beetles) mortality
 702 frameworks: -19.5 ± 2.7 tC.ha⁻¹, -3.7 ± 0.7 tC.ha⁻¹ and 9.3 ± 0.2 tC.ha⁻¹ for the abrupt, abrupt, no beetles and continuous

703 mortality frameworks, respectively. These differences were statistically significant (Wilcoxon, p -value<0001),
704 indicating a substantial initial reduction in NBP with the 'Abrupt' models, as ecosystems behaved as carbon sources,
705 whereas under the 'Continuous' model, they acted as carbon sinks (Fig. 8). The variability in NBP demonstrated the
706 broad temperature gradient in Europe and indicated that despite many locations potentially acting as sources under
707 the 'Abrupt' framework, some may transition to carbon sinks within the first 20 years following a disturbance.

708

709 Moving to the 50-years horizon, the difference between the three frameworks decreased, with net biome productions
710 of -3.8 ± 1.6 , 11.7 ± 0.4 and 14.9 ± 0.5 $\text{tC}\cdot\text{ha}^{-1}$ for the abrupt, abrupt, no beetles and continuous mortality frameworks,
711 respectively. The sink strength difference remained statistically significant (Wilcoxon, p -value<0.001), with the NBP
712 in the 'Abrupt' framework approaching carbon neutrality while without bark beetles outbreak ecosystems already
713 become a sink of carbon. The variability of responses depending on climatic conditions persisted, with the 'Abrupt'
714 framework showing a greater range compared to the 'Continuous' one. Some locations transitioned from carbon
715 sources to carbon sinks under the 'Continuous' framework, indicating a more resilient and gradual recovery in
716 ecosystem productivity (Fig. 8).

717

718 At the 100-years mark, the average accumulated NBP for the 'Abrupts' and 'Continuous' frameworks became much
719 closer (Wilcoxon, p -value<0.001), with values of 12.6 ± 0.7 , 18.9 ± 0.5 and 19.9 ± 1.2 $\text{tC}\cdot\text{ha}^{-1}$, respectively (Fig. 8). The
720 data showed a return to positive Cumulative NBP values, suggesting a long-term recovery and potential return to
721 pre-disturbance productivity levels within the century following the windthrow events. The 'continuous' model
722 version displayed a consistently higher median value, suggesting a more resilient recovery over the long term.

723

724 5. Discussion

725 5.1. Simulating the dynamics of bark beetle outbreaks and their interaction with windthrow

726 Our Bark beetle outbreak model formulation has demonstrated its capability to simulate a broad range of disturbance
727 dynamics. The variation in the outbreak dynamics and the response of the outbreak to its main drivers (Fig. 5 & 6)
728 give confidence in the ability of ORCHIDEE to simulate various outbreak scenarios observed across the temperate
729 and boreal zones under changing climate conditions.

730

731 Windthrow events have significant ecological maining because such disturbances offer fresh breeding substrates,
732 which in turn increase bark beetle populations (Lausch et al., 2011). Our modeling results align with these findings,
733 indicating that windthrows causing damage of 5% or more may trigger beetle outbreaks (Fig. 6). Additionally,
734 Wermelinger (2004) reported a strong increase in bark beetle populations post-windthrow, a pattern that our
735 ORCHIDEE simulations also reflect. The model pinpoints a buildup stage—spanning 1 to 9 years, where bark beetle
736 numbers increase prior to peaking, with the duration influenced by the severity of the windthrow and the prevailing
737 climate (Fig. 6).

738

739 Temperature is another critical factor affecting bark beetle life cycles. Studies by Benz et al. (2005) have highlighted
740 how intra- and interannual variation in temperature impact bark beetles, with warmer conditions fostering multiple
741 generations per year, whereas cooler, damp climates slow breeding and survival rates. In line with these findings,
742 ORCHIDEE's temperature-dependent simulations show variations in bark beetle impacts across different sites; cold
743 winters at locations such as SOR and REN reduced bark beetle activity compared to warmer sites like THA and
744 WET (Fig. 6). Lieutier et al. (2004) documented that significant bark beetle numbers can trigger mass attacks on
745 healthy trees. Our model incorporates this dynamic, illustrated by epidemic stages where living trees become viable
746 hosts, which then exacerbates the growth of the beetle population.

747

748 The aftermath of windthrow and subsequent bark beetle infestations also affects the forest carbon and nitrogen
749 cycles. This impact is observed in the form of snags—standing dead trees that undergo decomposition. As Rhoades,
750 (2019) observed, this can disrupt the link between soil and ecosystem carbon and nitrogen dynamics, a point echoed
751 by (Custer et al., 2020). While ORCHIDEE models the decay of fallen logs, it does not account for snags.
752 Nevertheless, the model suggests a recovery period ranging from 5 to 15 years, contingent upon the intensity of the
753 bark beetle outbreak (Fig. 7). As snags create gaps in the canopy, conditions favorable to natural forest regeneration
754 emerge, corroborating the affirmation of Jonášová and Prach, 2004. The ORCHIDEE model forecasts an increase in
755 tree recruitment due to the sharp reduction in stand density, allowing more sunlight to penetrate to the forest floor,
756 thereby stimulating growth (Fig. 7).

757

758 **5.2. Emerging property from interacting disturbances**

759 While this study hasn't provided a precise quantification of the impact of incorporating abrupt mortality versus a
760 fixed continuous background mortality, it demonstrated that the impact of abrupt mortality can vary across locations
761 and over time, i.e., ecosystem functions, such as carbon storage, are affected by natural disasters like pest outbreaks,
762 having significant impacts on short-to-mid-term carbon balance estimates. The simulation experiments also
763 highlighted that the legacy effects of disturbances can endure for decades, even for a simplified representation of
764 forest ecosystems such as ORCHIDEE, where the recovery might be too fast due to the absence of snags (Senf et al.,
765 2017).

766

767 The ability to simulate resistance as an emerging property is evident from Fig. 6 and 7 for locations REN, where no
768 bark beetle outbreaks were observed following a medium windthrow event (5%-20%). However, in all simulated
769 locations that couldn't resist a bark beetle outbreak, the forest was resilient and ecosystem functions were restored to
770 the level from before the windthrow. The elasticity of, e.g., the carbon sink capacity ranged from 7 to 14 years. This
771 elasticity is in line with current observational evidence from Millar and Stephenson, 2015 who found very little
772 evidence of ecosystem shifts due to natural disturbances in forests. Finally, after the disturbance and the recovery of
773 vegetation structure, the ecosystems simulated by ORCHIDEE showed persistence, i.e. the ability to continue along
774 their initial developmental path. In this study we follow the definitions of Grimm and Wissel, 1997 for resistance,
775 resilience, elasticity, and persistence.

776

777 **5.3. Are cascading disturbances important for carbon balance estimates ?**

778 The enhanced complexity introduced into the ORCHIDEE model by incorporating abrupt mortality events, as
779 opposed to a fixed-rate continuous mortality, prompts the question: does this model refinement yield significant new
780 insights into carbon balance estimates? Our century-long timeframe analysis demonstrates that the net biome
781 production (NBP; as defined in Chapin et al., 2006)—the metric for carbon balance—ultimately aligns between the
782 continuous and abrupt mortality frameworks, thereby affirming the model's capacity for convergence (Fig. 8). This
783 suggests that irrespective of the nature of the mortality events, the forest ecosystem exhibits a recovery phase,
784 marked by a growth boost that compensates for the growth deficits incurred during the disturbance.

785

786 Yet, our experiment has not taken into account the frequency of disturbances. Given the profound influence of
787 disturbance legacies on carbon dynamics, a recurrence interval shorter than the forest's recovery time might result in
788 a tipping point. Such a scenario could diminish the forest's carbon sequestration potential in the post-100-year
789 period, and in extreme cases, may even lead to ecosystem collapse—outcomes not explored in the current
790 simulations nor reflected in recent literature, such as the review by Millar and Stephenson (2015).

791

792 In the mid-term, spanning 20 to 50 years, the widely used continuous mortality model appears to inflate the carbon
793 sink capabilities of forests when juxtaposed with abrupt mortality scenarios. Since policy frameworks, including the
794 Green Deal for Europe (2023) and the Paris Agreement | CCNUCC (2023), often hinged upon these medium-term
795 predictions, they would benefit from adopting model simulations that integrate abrupt mortality events to avoid an
796 overestimation of forests' carbon sink capacities. Furthermore, the accuracy of carbon balance estimates strongly
797 depends upon the initial state of the forest in the model. Forest conditions markedly affect carbon uptake rates. Thus,
798 incorporating an abrupt mortality framework into the ORCHIDEE model could substantially refine and fortify the
799 predictive power of our carbon balance assessments across short, medium, and long-term scales.

800

801 **5.4. Shortcomings of the bark beetle outbreak model**

802 The bark beetle outbreak module developed in this study builds upon the strengths of the previously established
803 LandClim model, though it also inherited some of its limitations. One notable shortcoming is the module for beetle
804 phenology, which is an empirical model making use of accumulated degrees-days. Since the module's conception a
805 decade ago, Europe's climate has undergone substantial changes, primarily manifested in warmer winters and
806 springs (Copernicus, 2024). Because of these changes, chances have increased for two or even more bark beetle
807 generations within a calendar year (Hlásny et al., 2021a). These changes call for an update of the beetle's phenology
808 model to align with these more recent observations (Ogris et al., 2019).

809

810 A second limitation is that our study, ORCHIDEE, has been parameterized to simulate only *Ips Typographus* in
811 Europe. In order to change the Beetles/trees hosts ecosystem e.g. pine bark beetle in North America (*Dendroctonus*
812 *monticolae* Hopkins), the sensitivity of indexes must be revised, for example pine beetle is not breeding on the dead

813 wood falling from withrow but very sensitive to drought event(Preisler et al., 2012). $i_{\text{hosts defense}}$ and $i_{\text{hosts dead}}$ as well as
814 the phenology model will need to be revised.

815

816 Another issue is the model's consideration of drought. As outlined in the method section, drought is treated as an
817 exacerbating factor, rather than a primary trigger as is the case for windthrow. This understanding was accurate a
818 decade ago (Temperli et al., 2013); however, emerging evidence increasingly suggests that drought events may
819 indeed trigger bark beetle outbreaks across Europe (Netherer et al., 2015; Nardi et al., 2023). Consequently, this
820 extreme drought as a trigger should be incorporated in a future revision of ORCHIDEE's bark beetle outbreak
821 module.

822

823 **6. Outlook**

824 This study simulated how windthrow interacts with bark beetle infestations in unmanaged forests. Future research
825 will incorporate additional interactions, such as: the interplay between droughts, storms, and bark beetles; storms,
826 bark beetles, and fires; as well as forest management, storms, and bark beetles.

827

828 The bark beetle outbreak module could also be enhanced by simulating: (a) standing dead trees (or snags), which
829 would help account for differences in wood decomposition between snags and logs (Angers et al., 2012; Storaunet et
830 al., 2005), (b) the migration of bark beetles to neighboring locations, which becomes significant to account for in a
831 model that operates at spatial resolutions below approximately 10 kilometers, and (c) an up-to-date beetle phenology
832 module which accounts for the recent change in their behavior induced by climate change.

833

834 This research provides an initial qualitative assessment of a new model feature. However, the application of the
835 model necessitates an evaluation of the simulations against observations of cascading disturbances at the regional
836 scale, which is the topic of an ongoing study.

837

838 **7. Conclusion**

839 Our approach enables improving the realism of the bark beetle model in ORCHIDEE without reducing its generality
840 (Levins, 1966). The integration of a bark beetle outbreak module in interaction with other natural disturbance such
841 as windthrow into the ORCHIDEE land surface model has resulted in a broader range of disturbance dynamics and
842 has demonstrated ORCHIDEE's capacity to simulate various disturbance interaction scenarios under different
843 climatic conditions. Incorporating abrupt mortality events instead of a fixed continuous mortality calculation
844 provided new insights into carbon balance estimates. The study showed that the continuous mortality framework,
845 which is commonly used in the land-surface modeling community, tends to overestimate the carbon sink capacity of
846 forests in the 20 to 50 year range in ecosystems under high disturbance pressure, compared to scenarios with abrupt
847 mortality events.

848

849 Apart from these advances, the study revealed possible shortcomings in the bark beetle outbreak model including

850 the need to update the beetle's phenology model to reflect recent climate changes, and the need to consider extreme
851 drought as a trigger for bark beetle outbreaks in line with emerging evidence. Looking ahead, future work will
852 further develop the capability of ORCHIDEE to simulate interacting disturbances such as the interplay between
853 extreme droughts, storms, and bark beetles, and between storms, bark beetles, and fires.

854 The final step would be to realize a complete quantitative evaluation based on observation data such as produced by
855 (Marini et al., 2017) in order to assess the capability of ORCHIDEE to simulate complex interaction between
856 multiple sources of tree mortality affecting the carbon balance at large scale.

857

858 **8. Code availability**

859 • R script and data are available at :

860 <https://doi.org/10.5281/zenodo.8004954> or DOI <https://doi.org/10.5281/zenodo.8004954>

861 • ORCHIDEE rev 7791 code is also available from:

862 https://forge.ipsl.jussieu.fr/orchidee/browser/branches/publications/ORCHIDEE_gmd-2023-05

863

864 **9. Data availability**

865 • The Fluxnet climate forcing data are available at <https://fluxnet.org/>

866 • The simulation results use in this study are available at <https://doi.org/10.5281/zenodo.8004954>

867

868 **10. Author contribution**

869 G. Marie, S. Luyssaert designed the experiments and G. Marie conducted them. Following discussions with H.

870 Jactel, G. Petter and M. Cailleret, G. Marie developed the bark beetles model code and performed the simulations. J.

871 Jeong integrated the wind damage and bark beetle modules with each other. G. Marie, J. Jeong, V. Bastrikov, J.

872 Ghattas, B. Guenet, A.S. Lansø, M.J. McGrath, K. Naudts, A. Valade, C. Yue, and S. Luyssaert, contributed to the

873 development, parameterization and evaluation of the ORCHIDEE revision used in this study. G. Marie, J. Jeong, and

874 S. Luyssaert prepared the manuscript with contributions from all co-authors.

875

876 **11. Competing interests**

877 No competing interest

878

879 **12. Acknowledgements**

880 GM was funded by MSCF (CLIMPRO) and ADEME (DIPROG). SL and KN were funded by Horizon 2020,

881 HoliSoils (SEP-210673589) and Horizon Europe INFORMA (101060309). JJ was funded by Horizon 2020,

882 HoliSoils (SEP-210673589). BG was funded by Horizon 2020, HoliSoils (SEP-210673589). GP acknowledges

883 funding by the Swiss National Science Foundation (SNF 163250). ASL was funded by Horizon 2020, Crescendo

884 (641816). C.Y. was funded by the National Science Foundation of China (U20A2090 and 41971132). MJM was

885 supported by the European Commission, Horizon 2020 Framework Programme (VERIFY, grant no. 776810) and the

886 European Union's Horizon 2020 research and innovation programme under Grant Agreement No. 958927 (CoCO2).

887 AV acknowledges funding by Agropolis Fondation (2101-048). This work was performed using HPC resources
888 from GENCI-TGCC (Grant 2022-06328). The Textual AI - Open AI GPT4 (<https://chat.openai.com/>) has been used
889 for language editing at an early stage of manuscript preparation.

890

891 13. References

- 892 Abramowitz, G., Leuning, R., Clark, M., and Pitman, A.: Evaluating the Performance of Land Surface Models, *J.*
893 *Clim.*, 21, 5468–5481, <https://doi.org/10.1175/2008JCLI2378.1>, 2008.
- 894 Allen, C. D., Breshears, D. D., and McDowell, N. G.: On underestimation of global vulnerability to tree mortality
895 and forest die-off from hotter drought in the Anthropocene, *Ecosphere*, 6, art129,
896 <https://doi.org/10.1890/ES15-00203.1>, 2015.
- 897 Andrus, R. A., Hart, S. J., and Veblen, T. T.: Forest recovery following synchronous outbreaks of spruce and western
898 balsam bark beetle is slowed by ungulate browsing, *Ecology*, 101, e02998, <https://doi.org/10.1002/ecy.2998>,
899 2020.
- 900 Angers, V. A., Drapeau, P., and Bergeron, Y.: Mineralization rates and factors influencing snag decay in four North
901 American boreal tree species, *Can. J. For. Res.*, 42, 157–166, <https://doi.org/10.1139/x11-167>, 2012.
- 902 European State of the Climate | Copernicus: <https://climate.copernicus.eu/ESOTC>, last access: 25 March 2024.
- 903 Bakke, A.: The recent *Ips typographus* outbreak in Norway - experiences from a control program, *Ecography*, 12,
904 515–519, <https://doi.org/10.1111/j.1600-0587.1989.tb00930.x>, 1989.
- 905 Bentz, B. J., Régnière, J., Fettig, C. J., Hansen, E. M., Hayes, J. L., Hicke, J. A., Kelsey, R. G., Negrón, J. F., and
906 Seybold, S. J.: Climate Change and Bark Beetles of the Western United States and Canada: Direct and Indirect
907 Effects, *BioScience*, 60, 602–613, <https://doi.org/10.1525/bio.2010.60.8.6>, 2010.
- 908 Berner, L. T., Law, B. E., Meddens, A. J. H., and Hicke, J. A.: Tree mortality from fires, bark beetles, and timber
909 harvest during a hot and dry decade in the western United States (2003–2012), *Environ. Res. Lett.*, 12, 065005,
910 <https://doi.org/10.1088/1748-9326/aa6f94>, 2017.
- 911 Berryman, A. A.: *Population Cycles: The Case for Trophic Interactions*, Oxford University Press, 207 pp., 2002.
- 912 Biedermann, P. H. W., Müller, J., Grégoire, J.-C., Gruppe, A., Hagge, J., Hammerbacher, A., Hofstetter, R. W.,
913 Kandasamy, D., Kolarik, M., Kostovcik, M., Krokene, P., Sallé, A., Six, D. L., Turrini, T., Vanderpool, D.,
914 Wingfield, M. J., and Bässler, C.: Bark Beetle Population Dynamics in the Anthropocene: Challenges and
915 Solutions, *Trends Ecol. Evol.*, 34, 914–924, <https://doi.org/10.1016/j.tree.2019.06.002>, 2019.
- 916 Boucher, O., Servonnat, J., Albright, A. L., Aumont, O., Balkanski, Y., Bastrikov, V., Bekki, S., Bonnet, R., Bony,
917 S., Bopp, L., Braconnot, P., Brockmann, P., Cadule, P., Caubel, A., Cheruy, F., Codron, F., Cozic, A., Cugnet, D.,
918 D’Andrea, F., Davini, P., Laverigne, C. de, Denvil, S., Deshayes, J., Devilliers, M., Ducharne, A., Dufresne, J.-L.,
919 Dupont, E., Éthé, C., Fairhead, L., Falletti, L., Flavoni, S., Foujols, M.-A., Gardoll, S., Gastineau, G., Ghattas, J.,
920 Grandpeix, J.-Y., Guenet, B., Guez, L., E., Guilyardi, E., Guimberteau, M., Hauglustaine, D., Hourdin, F.,
921 Idelkadi, A., Joussaume, S., Kageyama, M., Khodri, M., Krinner, G., Lebas, N., Levavasseur, G., Lévy, C., Li,
922 L., Lott, F., Lurton, T., Luysaert, S., Madec, G., Madeleine, J.-B., Maignan, F., Marchand, M., Marti, O., Mellul,
923 L., Meurdesoif, Y., Mignot, J., Musat, I., Ottlé, C., Peylin, P., Planton, Y., Polcher, J., Rio, C., Rochetin, N.,
924 Rousset, C., Sepulchre, P., Sima, A., Swingedouw, D., Thiéblemont, R., Traore, A. K., Vancoppenolle, M., Vial,
925 J., Vialard, J., Viovy, N., and Vuichard, N.: Presentation and Evaluation of the IPSL-CM6A-LR Climate Model,
926 *J. Adv. Model. Earth Syst.*, 12, e2019MS002010, <https://doi.org/10.1029/2019MS002010>, 2020.
- 927 Bugmann, H. K. M.: A Simplified Forest Model to Study Species Composition Along Climate Gradients, *Ecology*,
928 77, 2055–2074, <https://doi.org/10.2307/2265700>, 1996.
- 929 Buma, B.: Disturbance interactions: characterization, prediction, and the potential for cascading effects, *Ecosphere*,
930 6, art70, <https://doi.org/10.1890/ES15-00058.1>, 2015.
- 931 Chapin, F. S., Woodwell, G. M., Randerson, J. T., Rastetter, E. B., Lovett, G. M., Baldocchi, D. D., Clark, D. A.,
932 Harmon, M. E., Schimel, D. S., Valentini, R., Wirth, C., Aber, J. D., Cole, J. J., Goulden, M. L., Harden, J. W.,
933 Heimann, M., Howarth, R. W., Matson, P. A., McGuire, A. D., Melillo, J. M., Mooney, H. A., Neff, J. C.,
934 Houghton, R. A., Pace, M. L., Ryan, M. G., Running, S. W., Sala, O. E., Schlesinger, W. H., and Schulze, E.-D.:
935 Reconciling Carbon-cycle Concepts, Terminology, and Methods, *Ecosystems*, 9, 1041–1050,
936 <https://doi.org/10.1007/s10021-005-0105-7>, 2006.
- 937 Chen, Y., Ryder, J., Bastrikov, V., McGrath, M. J., Naudts, K., Otto, J., Ottlé, C., Peylin, P., Polcher, J., Valade, A.,
938 Black, A., Elbers, J. A., Moors, E., Foken, T., van Gorsel, E., Haverd, V., Heinesch, B., Tiedemann, F., Knohl,
939 A., Launiainen, S., Loustau, D., Ogée, J., Vessala, T., and Luysaert, S.: Evaluating the performance of land

940 surface model ORCHIDEE-CAN v1.0 on water and energy flux estimation with a single- and multi-layer energy
941 budget scheme, *Geosci. Model Dev.*, 9, 2951–2972, <https://doi.org/10.5194/gmd-9-2951-2016>, 2016.

942 Chen, Y.-Y., Gardiner, B., Pasztor, F., Blennow, K., Ryder, J., Valade, A., Naudts, K., Otto, J., McGrath, M. J.,
943 Planque, C., and Luysaert, S.: Simulating damage for wind storms in the land surface model ORCHIDEE-CAN
944 (revision 4262), *Geosci. Model Dev.*, 11, 771–791, <https://doi.org/10.5194/gmd-11-771-2018>, 2018.

945 Ciais, P., Reichstein, M., Viovy, N., Granier, A., Ogée, J., Allard, V., Aubinet, M., Buchmann, N., Bernhofer, C.,
946 Carrara, A., Chevallier, F., De Noblet, N., Friend, A. D., Friedlingstein, P., Grünwald, T., Heinesch, B., Keronen,
947 P., Knohl, A., Krinner, G., Loustau, D., Manca, G., Matteucci, G., Miglietta, F., Ourcival, J. M., Papale, D.,
948 Pilegaard, K., Rambal, S., Seufert, G., Soussana, J. F., Sanz, M. J., Schulze, E. D., Vesala, T., and Valentini, R.:
949 Europe-wide reduction in primary productivity caused by the heat and drought in 2003, *Nature*, 437, 529–533,
950 <https://doi.org/10.1038/nature03972>, 2005.

951 Cox, P. M., Betts, R. A., Jones, C. D., Spall, S. A., and Totterdell, I. J.: Acceleration of global warming due to
952 carbon-cycle feedbacks in a coupled climate model, *Nature*, 408, 184–187, <https://doi.org/10.1038/35041539>,
953 2000.

954 Custer, G. F., van Diepen, L. T. A., and Stump, W. L.: Structural and Functional Dynamics of Soil Microbes
955 following Spruce Beetle Infestation, *Appl. Environ. Microbiol.*, 86, e01984-19,
956 <https://doi.org/10.1128/AEM.01984-19>, 2020.

957 Das, A. J., Stephenson, N. L., and Davis, K. P.: Why do trees die? Characterizing the drivers of background tree
958 mortality, *Ecology*, 97, 2616–2627, <https://doi.org/10.1002/ecy.1497>, 2016.

959 Deleuze, C., Pain, O., Dhôte, J.-F., and Hervé, J.-C.: A flexible radial increment model for individual trees in pure
960 even-aged stands, *Ann. For. Sci.*, 61, 327–335, <https://doi.org/10.1051/forest:2004026>, 2004.

961 Edburg, S. L., Hicke, J. A., Brooks, P. D., Pendall, E. G., Ewers, B. E., Norton, U., Gochis, D., Gutmann, E. D., and
962 Meddens, A. J.: Cascading impacts of bark beetle-caused tree mortality on coupled biogeophysical and
963 biogeochemical processes, *Front. Ecol. Environ.*, 10, 416–424, <https://doi.org/10.1890/110173>, 2012.

964 Friedlingstein, P., Cox, P., Betts, R., Bopp, L., Bloh, W. von, Brovkin, V., Cadule, P., Doney, S., Eby, M., Fung, I.,
965 Bala, G., John, J., Jones, C., Joos, F., Kato, T., Kawamiya, M., Knorr, W., Lindsay, K., Matthews, H. D.,
966 Raddatz, T., Rayner, P., Reick, C., Roeckner, E., Schnitzler, K.-G., Schnur, R., Strassmann, K., Weaver, A. J.,
967 Yoshikawa, C., and Zeng, N.: Climate–Carbon Cycle Feedback Analysis: Results from the C4MIP Model
968 Intercomparison, *J. Clim.*, 19, 3337–3353, <https://doi.org/10.1175/JCLI3800.1>, 2006.

969 Grimm, V. and Wissel, C.: Babel, or the ecological stability discussions: an inventory and analysis of terminology
970 and a guide for avoiding confusion, *Oecologia*, 109, 323–334, <https://doi.org/10.1007/s004420050090>, 1997.

971 Havašová, M., Ferencík, J., and Jakuš, R.: Interactions between windthrow, bark beetles and forest management in
972 the Tatra national parks, *For. Ecol. Manag.*, 391, 349–361, <https://doi.org/10.1016/j.foreco.2017.01.009>, 2017.

973 Haverd, V., Lovell, J. L., Cuntz, M., Jupp, D. L. B., Newnham, G. J., and Sea, W.: The Canopy Semi-analytic Pgap
974 And Radiative Transfer (CanSPART) model: Formulation and application, *Agric. For. Meteorol.*, 160, 14–35,
975 <https://doi.org/10.1016/j.agrformet.2012.01.018>, 2012.

976 Hicke, J. A., Allen, C. D., Desai, A. R., Dietze, M. C., Hall, R. J., Hogg, E. H., Kashian, D. M., Moore, D., Raffa, K.
977 F., Sturrock, R. N., and Vogelmann, J.: Effects of biotic disturbances on forest carbon cycling in the United
978 States and Canada., <https://doi.org/10.1111/j.1365-2486.2011.02543.x>, 2012.

979 Hlásny, T., König, L., Krokene, P., Lindner, M., Montagné-Huck, C., Müller, J., Qin, H., Raffa, K. F., Schelhaas,
980 M.-J., Svoboda, M., Viiri, H., and Seidl, R.: Bark Beetle Outbreaks in Europe: State of Knowledge and Ways
981 Forward for Management, *Curr. For. Rep.*, 7, 138–165, <https://doi.org/10.1007/s40725-021-00142-x>, 2021a.

982 Hlásny, T., Zimová, S., Merganičová, K., Štěpánek, P., Modlinger, R., and Turčáni, M.: Devastating outbreak of bark
983 beetles in the Czech Republic: Drivers, impacts, and management implications, *For. Ecol. Manag.*, 490, 119075,
984 <https://doi.org/10.1016/j.foreco.2021.119075>, 2021b.

985 Huang, J., Kautz, M., Trowbridge, A. M., Hammerbacher, A., Raffa, K. F., Adams, H. D., Goodsman, D. W., Xu, C.,
986 Meddens, A. J. H., Kandasamy, D., Gershenson, J., Seidl, R., and Hartmann, H.: Tree defence and bark beetles in
987 a drying world: carbon partitioning, functioning and modelling, *New Phytol.*, 225, 26–36,
988 <https://doi.org/10.1111/nph.16173>, 2020.

989 Jonášová, M. and Prach, K.: Central-European mountain spruce (*Picea abies* (L.) Karst.) forests: regeneration of tree
990 species after a bark beetle outbreak, *Ecol. Eng.*, 23, 15–27, <https://doi.org/10.1016/j.ecoleng.2004.06.010>, 2004.

991 Jönsson, A. M., Schroeder, L. M., Lagergren, F., Anderbrant, O., and Smith, B.: Guess the impact of *Ips*
992 *typographus*—An ecosystem modelling approach for simulating spruce bark beetle outbreaks, *Agric. For.*
993 *Meteorol.*, 166–167, 188–200, <https://doi.org/10.1016/j.agrformet.2012.07.012>, 2012.

994 Kärvmö, S. and Schroeder, L. M.: A comparison of outbreak dynamics of the spruce bark beetle in Sweden and the
995 mountain pine beetle in Canada (Curculionidae: Scolytinae), 2010.

996 Kautz, M., Anthoni, P., Meddens, A. J. H., Pugh, T. A. M., and Arneeth, A.: Simulating the recent impacts of multiple
997 biotic disturbances on forest carbon cycling across the United States, *Glob. Change Biol.*, 24, 2079–2092,
998 <https://doi.org/10.1111/gcb.13974>, 2018.

999 Komonen, A., Schroeder, L. M., and Weslien, J.: *Ips typographus* population development after a severe storm in a
1000 nature reserve in southern Sweden, *J. Appl. Entomol.*, 135, 132–141,
1001 <https://doi.org/10.1111/j.1439-0418.2010.01520.x>, 2011.

1002 Krinner, G., Viovy, N., de Noblet-Ducoudré, N., Ogée, J., Polcher, J., Friedlingstein, P., Ciais, P., Sitch, S., and
1003 Prentice, I. C.: A dynamic global vegetation model for studies of the coupled atmosphere-biosphere system:
1004 DVGCM FOR COUPLED CLIMATE STUDIES, *Glob. Biogeochem. Cycles*, 19,
1005 <https://doi.org/10.1029/2003GB002199>, 2005.

1006 Kurz, W. A., Dymond, C. C., Stinson, G., Rampley, G. J., Neilson, E. T., Carroll, A. L., Ebata, T., and Safranyik, L.:
1007 Mountain pine beetle and forest carbon feedback to climate change, *Nature*, 452, 987–990,
1008 <https://doi.org/10.1038/nature06777>, 2008a.

1009 Kurz, W. A., Dymond, C. C., Stinson, G., Rampley, G. J., Neilson, E. T., Carroll, A. L., Ebata, T., and Safranyik, L.:
1010 Mountain pine beetle and forest carbon feedback to climate change, *Nature*, 452, 987–990,
1011 <https://doi.org/10.1038/nature06777>, 2008b.

1012 Kurz, W. A., Stinson, G., Rampley, G. J., Dymond, C. C., and Neilson, E. T.: Risk of natural disturbances makes
1013 future contribution of Canada’s forests to the global carbon cycle highly uncertain, *Proc. Natl. Acad. Sci.*, 105,
1014 1551–1555, <https://doi.org/10.1073/pnas.0708133105>, 2008c.

1015 Lasslop, G., Thonicke, K., and Kloster, S.: SPITFIRE within the MPI Earth system model: Model development and
1016 evaluation, *J. Adv. Model. Earth Syst.*, 6, 740–755, <https://doi.org/10.1002/2013MS000284>, 2014.

1017 Lausch, A., Fahse, L., and Heurich, M.: Factors affecting the spatio-temporal dispersion of *Ips typographus* (L.) in
1018 Bavarian Forest National Park: A long-term quantitative landscape-level analysis, *For. Ecol. Manag.*, 261,
1019 233–245, <https://doi.org/10.1016/j.foreco.2010.10.012>, 2011.

1020 Levins, R.: The Strategy of Model Building in Population Biology, *Am. Sci.*, 54, 421–431, 1966.

1021 Lieutier, F.: Mechanisms of Resistance in Conifers and Bark beetle Attack Strategies, in: *Mechanisms and
1022 Deployment of Resistance in Trees to Insects*, edited by: Wagner, M. R., Clancy, K. M., Lieutier, F., and Paine, T.
1023 D., Springer Netherlands, Dordrecht, 31–77, https://doi.org/10.1007/0-306-47596-0_2, 2002.

1024 Lombardero, M. J., Ayres, M. P., Ayres, B. D., and Reeve, J. D.: Cold Tolerance of Four Species of Bark Beetle
1025 (Coleoptera: Scolytidae) in North America, *Environ. Entomol.*, 29, 421–432,
1026 <https://doi.org/10.1603/0046-225X-29.3.421>, 2000.

1027 Luyssaert, S., Marie, G., Valade, A., Chen, Y.-Y., Njakou Djomo, S., Ryder, J., Otto, J., Naudts, K., Lansø, A. S.,
1028 Ghattas, J., and McGrath, M. J.: Trade-offs in using European forests to meet climate objectives, *Nature*, 562,
1029 259–262, <https://doi.org/10.1038/s41586-018-0577-1>, 2018.

1030 Marini, L., Økland, B., Jönsson, A. M., Bentz, B., Carroll, A., Forster, B., Grégoire, J.-C., Hurling, R., Nageleisen,
1031 L. M., Netherer, S., Ravn, H. P., Weed, A., and Schroeder, M.: Climate drivers of bark beetle outbreak dynamics
1032 in Norway spruce forests, *Ecography*, 40, 1426–1435, <https://doi.org/10.1111/ecog.02769>, 2017.

1033 Mezei, P., Grodzki, W., Blaženec, M., and Jakuš, R.: Factors influencing the *wind-bark beetles’* disturbance system
1034 in the course of an *Ips typographus* outbreak in the Tatra Mountains, *For. Ecol. Manag.*, 312, 67–77,
1035 <https://doi.org/10.1016/j.foreco.2013.10.020>, 2014.

1036 Mezei, P., Jakuš, R., Pennerstorfer, J., Havašová, M., Škvarenina, J., Ferenčík, J., Slivinský, J., Bičárová, S., Bilčík,
1037 D., Blaženec, M., and Netherer, S.: Storms, temperature maxima and the Eurasian spruce bark beetle *Ips
1038 typographus*—An infernal trio in Norway spruce forests of the Central European High Tatra Mountains, *Agric.
1039 For. Meteorol.*, 242, 85–95, <https://doi.org/10.1016/j.agrformet.2017.04.004>, 2017.

1040 Migliavacca, M., Dosio, A., Kloster, S., Ward, D. S., Camia, A., Houborg, R., Houston Durrant, T., Khabarov, N.,
1041 Krasovskii, A. A., San Miguel-Ayanz, J., and Cescatti, A.: Modeling burned area in Europe with the Community
1042 Land Model, *J. Geophys. Res. Biogeosciences*, 118, 265–279, <https://doi.org/10.1002/jgrg.20026>, 2013.

1043 Migliavacca, M., Musavi, T., Mahecha, M. D., Nelson, J. A., Knauer, J., Baldocchi, D. D., Perez-Priego, O.,
1044 Christiansen, R., Peters, J., Anderson, K., Bahn, M., Black, T. A., Blanken, P. D., Bonal, D., Buchmann, N.,
1045 Caldararu, S., Carrara, A., Carvalhais, N., Cescatti, A., Chen, J., Cleverly, J., Cremonese, E., Desai, A. R.,
1046 El-Madany, T. S., Farella, M. M., Fernández-Martínez, M., Filippa, G., Forkel, M., Galvagno, M., Gomasasca,
1047 U., Gough, C. M., Göckede, M., Ibrom, A., Ikawa, H., Janssens, I. A., Jung, M., Kattge, J., Keenan, T. F., Knohl,
1048 A., Kobayashi, H., Kraemer, G., Law, B. E., Liddell, M. J., Ma, X., Mammarella, I., Martini, D., Macfarlane, C.,
1049 Matteucci, G., Montagnani, L., Pabon-Moreno, D. E., Panigada, C., Papale, D., Pendall, E., Penuelas, J., Phillips,
1050 R. P., Reich, P. B., Rossini, M., Rotenberg, E., Scott, R. L., Stahl, C., Weber, U., Wohlfahrt, G., Wolf, S., Wright,
1051 I. J., Yakir, D., Zaehle, S., and Reichstein, M.: The three major axes of terrestrial ecosystem function, *Nature*,

1052 598, 468–472, <https://doi.org/10.1038/s41586-021-03939-9>, 2021.

1053 Millar, C. I. and Stephenson, N. L.: Temperate forest health in an era of emerging megadisturbance, *Science*, 349,
1054 823–826, <https://doi.org/10.1126/science.aaa9933>, 2015.

1055 Morehouse, K., Johns, T., Kaye, J., and Kaye, M.: Carbon and nitrogen cycling immediately following bark beetle
1056 outbreaks in southwestern ponderosa pine forests, *For. Ecol. Manag.*, 255, 2698–2708,
1057 <https://doi.org/10.1016/j.foreco.2008.01.050>, 2008.

1058 Nardi, D., Jactel, H., Pagot, E., Samalens, J.-C., and Marini, L.: Drought and stand susceptibility to attacks by the
1059 European spruce bark beetle: A remote sensing approach, *Agric. For. Entomol.*, 25, 119–129,
1060 <https://doi.org/10.1111/afe.12536>, 2023.

1061 Naudts, K., Ryder, J., McGrath, M. J., Otto, J., Chen, Y., Valade, A., Bellasen, V., Berhongaray, G., Bönisch, G.,
1062 Campioli, M., and others: A vertically discretised canopy description for ORCHIDEE (SVN r2290) and the
1063 modifications to the energy, water and carbon fluxes, *Geosci. Model Dev.*, 8, 2035–2065, 2015a.

1064 Naudts, K., Ryder, J., McGrath, M. J., Otto, J., Chen, Y., Valade, A., Bellasen, V., Berhongaray, G., Bönisch, G.,
1065 Campioli, M., Ghattas, J., De Groote, T., Haverd, V., Kattge, J., MacBean, N., Maignan, F., Merilä, P., Penuelas,
1066 J., Peylin, P., Pinty, B., Pretzsch, H., Schulze, E. D., Solyga, D., Vuichard, N., Yan, Y., and Luyssaert, S.: A
1067 vertically discretised canopy description for ORCHIDEE (SVN r2290) and the modifications to the energy, water
1068 and carbon fluxes, *Geosci. Model Dev.*, 8, 2035–2065, <https://doi.org/10.5194/gmd-8-2035-2015>, 2015b.

1069 Naudts, K., Chen, Y., McGrath, M. J., Ryder, J., Valade, A., Otto, J., and Luyssaert, S.: Europe’s forest management
1070 did not mitigate climate warming, *Science*, 351, 597–600, <https://doi.org/10.1126/science.aad7270>, 2016.

1071 Netherer, S., Matthews, B., Katzensteiner, K., Blackwell, E., Henschke, P., Hietz, P., Pennerstorfer, J., Rosner, S.,
1072 Kikuta, S., Schume, H., and Schopf, A.: Do water-limiting conditions predispose Norway spruce to bark beetle
1073 attack?, *New Phytol.*, 205, 1128–1141, <https://doi.org/10.1111/nph.13166>, 2015.

1074 Ogris, N., Ferlan, M., Hauptman, T., Pavlin, R., Kavčič, A., Jurc, M., and de Groot, M.: RITY – A phenology model
1075 of *Ips typographus* as a tool for optimization of its monitoring, *Ecol. Model.*, 410, 108775,
1076 <https://doi.org/10.1016/j.ecolmodel.2019.108775>, 2019.

1077 Pastorello, G., Trotta, C., Canfora, E., Chu, H., Christianson, D., Cheah, Y.-W., Poindexter, C., Chen, J., Elbashandy,
1078 A., Humphrey, M., Isaac, P., Polidori, D., Reichstein, M., Ribeca, A., van Ingen, C., Vuichard, N., Zhang, L.,
1079 Amiro, B., Ammann, C., Arain, M. A., Ardö, J., Arkebauer, T., Arndt, S. K., Arriga, N., Aubinet, M., Aurela, M.,
1080 Baldocchi, D., Barr, A., Beamesderfer, E., Marchesini, L. B., Bergeron, O., Beringer, J., Bernhofer, C.,
1081 Berveiller, D., Billesbach, D., Black, T. A., Blanken, P. D., Bohrer, G., Boike, J., Bolstad, P. V., Bonal, D.,
1082 Bonnefond, J.-M., Bowling, D. R., Bracho, R., Brodeur, J., Brümmer, C., Buchmann, N., Burban, B., Burns, S.
1083 P., Buysse, P., Cale, P., Cavagna, M., Cellier, P., Chen, S., Chini, I., Christensen, T. R., Cleverly, J., Collalti, A.,
1084 Consalvo, C., Cook, B. D., Cook, D., Coursolle, C., Cremonese, E., Curtis, P. S., D’Andrea, E., da Rocha, H.,
1085 Dai, X., Davis, K. J., Cinti, B. D., Grandcourt, A. de Ligne, A. D., De Oliveira, R. C., Delpierre, N., Desai, A.
1086 R., Di Bella, C. M., Tommasi, P. di, Dolman, H., Domingo, F., Dong, G., Dore, S., Duce, P., Dufrêne, E., Dunn,
1087 A., Dušek, J., Eamus, D., Eichelmann, U., ElKhidir, H. A. M., Eugster, W., Ewenz, C. M., Ewers, B., Famulari,
1088 D., Fares, S., Feigenwinter, I., Feitz, A., Fensholt, R., Filippa, G., Fischer, M., Frank, J., Galvagno, M., et al.:
1089 The FLUXNET2015 dataset and the ONEFlux processing pipeline for eddy covariance data, *Sci. Data*, 7, 225,
1090 <https://doi.org/10.1038/s41597-020-0534-3>, 2020.

1091 Pasztor, F., Matulla, C., Rammer, W., and Lexer, M. J.: Drivers of the bark beetle disturbance regime in Alpine
1092 forests in Austria, *For. Ecol. Manag.*, 318, 349–358, <https://doi.org/10.1016/j.foreco.2014.01.044>, 2014.

1093 Pfeifer, E. M., Hicke, J. A., and Meddens, A. J. H.: Observations and modeling of aboveground tree carbon stocks
1094 and fluxes following a bark beetle outbreak in the western United States, *Glob. Change Biol.*, 17, 339–350,
1095 <https://doi.org/10.1111/j.1365-2486.2010.02226.x>, 2011.

1096 Pineau, X., David, G., Peter, Z., Sallé, A., Baude, M., Lieutier, F., and Jactel, H.: Effect of temperature on the
1097 reproductive success, developmental rate and brood characteristics of *Ips sexdentatus* (Boern.), *Agric. For.*
1098 *Entomol.*, 19, 23–33, <https://doi.org/10.1111/afe.12177>, 2017.

1099 Preisler, H. K., Hicke, J. A., Ager, A. A., and Hayes, J. L.: Climate and weather influences on spatial temporal
1100 patterns of mountain pine beetle populations in Washington and Oregon, *Ecology*, 93, 2421–2434,
1101 <https://doi.org/10.1890/11-1412.1>, 2012.

1102 Pugh, T. A. M., Jones, C. D., Huntingford, C., Burton, C., Arneth, A., Brovkin, V., Ciais, P., Lomas, M., Robertson,
1103 E., and Piao, S. L.: A Large Committed Long-Term Sink of Carbon due to Vegetation Dynamics, *Earths Future*,
1104 2017.

1105 Quillet, A., Peng, C., and Garneau, M.: Toward dynamic global vegetation models for simulating vegetation–climate
1106 interactions and feedbacks: recent developments, limitations, and future challenges, *Environ. Rev.*, 18, 333–353,
1107 <https://doi.org/10.1139/A10-016>, 2010.

1108 Raffa, K. F., Aukema, B. H., Bentz, B. J., Carroll, A. L., Hicke, J. A., Turner, M. G., and Romme, W. H.: Cross-scale
1109 Drivers of Natural Disturbances Prone to Anthropogenic Amplification: The Dynamics of Bark Beetle Eruptions,
1110 *BioScience*, 58, 501–517, <https://doi.org/10.1641/B580607>, 2008.

1111 Rhoades, C. C.: Soil Nitrogen Leaching in Logged Beetle-Killed Forests and Implications for Riparian Fuel
1112 Reduction, *J. Environ. Qual.*, 48, 305–313, <https://doi.org/10.2134/jeq2018.04.0169>, 2019.

1113 Ryder, J., Polcher, J., Peylin, P., Otlé, C., Chen, Y., van Gorsel, E., Haverd, V., McGrath, M. J., Naudts, K., Otto, J.,
1114 Valade, A., and Luyssaert, S.: A multi-layer land surface energy budget model for implicit coupling with global
1115 atmospheric simulations, *Geosci. Model Dev.*, 9, 223–245, <https://doi.org/10.5194/gmd-9-223-2016>, 2016.

1116 Schumacher, S.: The role of large-scale disturbances and climate for the dynamics of forested landscapes in the
1117 European Alps, Doctoral Thesis, ETH Zurich, <https://doi.org/10.3929/ethz-a-004818825>, 2004.

1118 Seidl, R. and Rammer, W.: Climate change amplifies the interactions between wind and bark beetle disturbances in
1119 forest landscapes, *Landsc. Ecol.*, 1–14, <https://doi.org/10.1007/s10980-016-0396-4>, 2016.

1120 Seidl, R., Fernandes, P. M., Fonseca, T. F., Gillet, F., Jönsson, A. M., Merganičová, K., Netherer, S., Arpacı, A.,
1121 Bontemps, J.-D., Bugmann, H., González-Olabarria, J. R., Lasch, P., Meredieu, C., Moreira, F., Schelhaas, M.-J.,
1122 and Mohren, F.: Modelling natural disturbances in forest ecosystems: a review, *Ecol. Model.*, 222, 903–924,
1123 <https://doi.org/10.1016/j.ecolmodel.2010.09.040>, 2011.

1124 Seidl, R., Schelhaas, M.-J., Rammer, W., and Verkerk, P. J.: Increasing forest disturbances in Europe and their
1125 impact on carbon storage, *Nat. Clim. Change*, 4, 806–810, <https://doi.org/10.1038/nclimate2318>, 2014.

1126 Seidl, R., Thom, D., Kautz, M., Martin-Benito, D., Peltoniemi, M., Vacchiano, G., Wild, J., Ascoli, D., Petr, M.,
1127 Honkaniemi, J., Lexer, M. J., Trotsiuk, V., Mairota, P., Svoboda, M., Fabrika, M., Nagel, T. A., and Reyer, C. P.
1128 O.: Forest disturbances under climate change, *Nat. Clim. Change*, 7, 395–402,
1129 <https://doi.org/10.1038/nclimate3303>, 2017.

1130 Seidl, R., Klöner, G., Rammer, W., Essl, F., Moreno, A., Neumann, M., and Dullinger, S.: Invasive alien pests
1131 threaten the carbon stored in Europe’s forests, *Nat. Commun.*, 9, 1626,
1132 <https://doi.org/10.1038/s41467-018-04096-w>, 2018.

1133 Senf, C., Pflugmacher, D., Hostert, P., and Seidl, R.: Using Landsat time series for characterizing forest disturbance
1134 dynamics in the coupled human and natural systems of Central Europe, *ISPRS J. Photogramm. Remote Sens.*,
1135 130, 453–463, <https://doi.org/10.1016/j.isprsjprs.2017.07.004>, 2017.

1136 Storaunet, K. O., Rolstad, J., Gjerde, I., and Gundersen, V. S.: Historical logging, productivity, and structural
1137 characteristics of boreal coniferous forests in Norway, *Silva Fenn.*, 39, 2005.

1138 Temperli, C., Bugmann, H., and Elkin, C.: Cross-scale interactions among bark beetles, climate change, and wind
1139 disturbances: a landscape modeling approach, *Ecol. Monogr.*, 83, 383–402, <https://doi.org/10.1890/12-1503.1>,
1140 2013a.

1141 Temperli, C., Bugmann, H., and Elkin, C.: Cross-scale interactions among bark beetles, climate change, and wind
1142 disturbances: a landscape modeling approach, *Ecol. Monogr.*, 83, 383–402, <https://doi.org/10.1890/12-1503.1>,
1143 2013b.

1144 Thurner, M., Beer, C., Ciais, P., Friend, A. D., Ito, A., Kleidon, A., Lomas, M. R., Quegan, S., Rademacher, T. T.,
1145 Schaphoff, S., Tum, M., Wiltshire, A., and Carvalhais, N.: Evaluation of climate-related carbon turnover
1146 processes in global vegetation models for boreal and temperate forests, *Glob. Change Biol.*, 23, 3076–3091,
1147 <https://doi.org/10.1111/gcb.13660>, 2017.

1148 Van Meerbeek, K., Jucker, T., and Svenning, J.-C.: Unifying the concepts of stability and resilience in ecology, *J.*
1149 *Ecol.*, 109, 3114–3132, <https://doi.org/10.1111/1365-2745.13651>, 2021.

1150 Vuichard, N., Messina, P., Luyssaert, S., Guenet, B., Zaehle, S., Ghattas, J., Bastrikov, V., and Peylin, P.: Accounting
1151 for carbon and nitrogen interactions in the global terrestrial ecosystem model ORCHIDEE (trunk version, rev
1152 4999): multi-scale evaluation of gross primary production, *Geosci. Model Dev.*, 12, 4751–4779,
1153 <https://doi.org/10.5194/gmd-12-4751-2019>, 2019.

1154 Wermelinger, B.: Ecology and management of the spruce bark beetle *Ips typographus*—a review of recent research,
1155 *For. Ecol. Manag.*, 202, 67–82, <https://doi.org/10.1016/j.foreco.2004.07.018>, 2004.

1156 Wichmann, L. and Ravn, H. P.: The spread of *Ips typographus* (L.) (Coleoptera, Scolytidae) attacks following heavy
1157 windthrow in Denmark, analysed using GIS, *For. Ecol. Manag.*, 148, 31–39,
1158 [https://doi.org/10.1016/S0378-1127\(00\)00477-1](https://doi.org/10.1016/S0378-1127(00)00477-1), 2001.

1159 Yao, Y., Joetzer, E., Ciais, P., Viovy, N., Cresto Aleina, F., Chave, J., Sack, L., Bartlett, M., Meir, P., Fisher, R., and
1160 Luyssaert, S.: Forest fluxes and mortality response to drought: model description (ORCHIDEE-CAN-NHA
1161 r7236) and evaluation at the Caxiuana drought experiment, *Geosci. Model Dev.*, 15, 7809–7833,
1162 <https://doi.org/10.5194/gmd-15-7809-2022>, 2022.

1163 Yi-Ying, C., Gardiner, B., Pasztor, F., Blennow, K., Ryder, J., Valade, A., Naudts, K., Otto, J., McGrath, M. J., and

1164 Planque, C.: Simulating damage for wind storms in the land surface model ORCHIDEE-CAN (revision 4262),
1165 Geosci. Model Dev., 11, 771, 2018.

1166 Yue, C., Ciais, P., Cadule, P., Thonicke, K., Archibald, S., Poulter, B., Hao, W. M., Hantson, S., Mouillot, F.,
1167 Friedlingstein, P., Maignan, F., and Viovy, N.: Modelling the role of fires in the terrestrial carbon balance by
1168 incorporating SPITFIRE into the global vegetation model ORCHIDEE – Part 1: simulating historical global
1169 burned area and fire regimes, Geosci. Model Dev., 7, 2747–2767, <https://doi.org/10.5194/gmd-7-2747-2014>,
1170 2014.

1171 Zaehle, S. and Dalmonech, D.: Carbon–nitrogen interactions on land at global scales: current understanding in
1172 modelling climate biosphere feedbacks, Curr. Opin. Environ. Sustain., 3, 311–320,
1173 <https://doi.org/10.1016/j.cosust.2011.08.008>, 2011.

1174 Zaehle, S. and Friend, A. D.: Carbon and nitrogen cycle dynamics in the O-CN land surface model: 1. Model
1175 description, site-scale evaluation, and sensitivity to parameter estimates, Glob. Biogeochem. Cycles, 24,
1176 <https://doi.org/10.1029/2009GB003521>, 2010.

1177 Zhang, Q.-H. and Schlyter, F.: Olfactory recognition and behavioural avoidance of angiosperm nonhost volatiles by
1178 conifer-inhabiting bark beetles, Agric. For. Entomol., 6, 1–20, <https://doi.org/10.1111/j.1461-9555.2004.00202.x>,
1179 2004.

1180 Zscheischler, J., Westra, S., van den Hurk, B. J. J. M., Seneviratne, S. I., Ward, P. J., Pitman, A., AghaKouchak, A.,
1181 Bresch, D. N., Leonard, M., Wahl, T., and Zhang, X.: Future climate risk from compound events, Nat. Clim.
1182 Change, 8, 469–477, <https://doi.org/10.1038/s41558-018-0156-3>, 2018.

1183